Genome of the estuarine oyster provides insights into climate impact and adaptive plasticity

Subtitle: Insights into climate impact and adaptive plasticity

Ao Li[1,2,3†], He Dai[4†], Ximing Guo[5†], Ziyan Zhang[1,6], Kexin Zhang[1,6], Chaogang Wang[1,6], Wei Wang[1,3,7], Hongju Chen[4], Xumin Li[4], Hongkun Zheng[4], Guofan Zhang[1,3,7*] and Li Li[1,2,3*]

[1]CAS and Shandong Province Key Laboratory of Experimental Marine Biology, Center for Ocean Mega-Science, Institute of Oceanology, Chinese Academy of Sciences, Qingdao, China. [2]Laboratory for Marine Fisheries Science and Food Production Processes, Pilot National Laboratory for Marine Science and Technology, Qingdao, China. [3]National and Local Joint Engineering Key Laboratory of Ecological Mariculture, Institute of Oceanology, Chinese Academy of Sciences, Qingdao, China. [4]Biomarker Technologies Corporation, Beijing, China. [5]Haskin Shellfish Research Laboratory, Department of Marine and Coastal Sciences, Rutgers University, Port Norris, NJ, USA. [6]University of Chinese Academy of Sciences, Beijing, China. [7]Laboratory for Marine Biology and Biotechnology, Pilot National Laboratory for Marine Science and Technology, Qingdao, China. [†]These authors contributed equally: A. Li, H. Dai and X. Guo. [*]e-mail: lili@qdio.ac.cn and gzhang@qdio.ac.cn

Abstract

Understanding the roles of genetic divergence and phenotypic plasticity in adaptation is central to evolutionary biology and important for assessing adaptive potential of species under climate change. Analysis of a chromosome-level assembly and resequencing of individuals across wide latitude distribution in the estuarine oyster (*Crassostrea ariakensis*) revealed unexpectedly low genomic diversity and population structures shaped by historical glaciation, geological events and oceanographic forces. Strong selection signals were detected in genes responding to temperature and salinity stress, especially of the expanded *solute carrier* families, highlighting the significance of gene expansion in environmental adaptation. Genes exhibiting high plasticity showed strong selection in upstream regulatory regions that modulate transcription, indicating selection favoring plasticity. Our findings suggest that genomic variation and population structure in marine bivalves are heavily influenced by climate history and physical forces, and gene expansion and selection may enhance phenotypic plasticity that is critical for the adaptation to rapidly changing environments.

Climate change poses a serious threat to global biodiversity and the stability of ecosystems. Oceans bear the blunt of climate change as they absorb most of the energy and about one-third of the carbon dioxide created by human activities (*1*). World oceans become warmer and more acidic. Sea levels are rising, and ocean circulation patterns are changing. With the rising of global temperature, dry regions are getting drier, while wet regions become wetter (*2*), increasing salinity difference among estuaries (*3*). These rapid changes in world's oceans are having a significant impact on marine ecosystems, much of which remains poorly understood. The impact may vary among different organisms, and changes in keystone species may have a large effect on stability of an ecosystem. Understanding how organisms adapt to environmental shifts is fundamental to evolutionary biology and critical in assessing their adaptive potential under climate change.

The ability of an organism to survive and adapt to sudden environmental changes depends on available genetic variation and phenotypic plasticity. The standing genetic variation of a species is the outcome of its evolutionary history shaped by mutation, selection and genetic drifts (*4-6*). Past and on-going climate and geological events may leave signatures of selection or bottleneck in the genome and influence the geographic distribution of genetic variation (*7-9*). Many recent studies have revealed the significance of phenotypic plasticity in environmental adaptation (*10-15*). Phenotypic plasticity may buffer against sudden environmental changes and provides time for adaptation to occur (*10, 13, 14, 16*). Phenotypic plasticity is particularly pronounced and important for sessile organisms inhabiting estuarine and intertidal zones that cannot use avoidance to cope with wide fluctuations in environmental conditions (*10, 11, 17*), although the genetic basis of the enhanced plasticity is not clear (*18, 19*).

Oysters are keystone species in coastal and estuarine ecology providing critical ecological services as filter-feeders and habitat engineers. As sessile bivalves thriving in the coastal zone, oysters are well adapted to highly dynamic environmental conditions, as reflected in their high genetic diversity and plasticity (*10, 20-23*),

making them interesting models for studying responses to climate change. In addition to threats from climate change, oyster populations worldwide have been decimated by over-fishing, habitat destruction and infectious diseases (*24*, *25*). The estuarine (Jinjiang or Suminoe) oyster (*Crassostrea ariakensis*, Fig. 1a) is broadly distributed in estuaries of East Asia over large latitude and experiences wide ranges of temperature and salinity (*26-28*). Unlike the Pacific oyster (*Crassostrea gigas*), a sympatric sister-species that is highly abundant in high-salinity waters of higher latitude, the estuarine oyster is only found in estuaries at low abundance within its wide distribution range. The evolutionary pathways leading to the stark differences in abundance, distribution and salinity preference are not clear but important to our understanding of adaptive evolution.

While genetic changes can be inferred with genetic markers, whole-genome analysis is essential for exploring all genetic variation and identifying genes and selection events that are critical for adaption. Using multi-omic analyses, we previously showed that the Pacific oyster has a highly polymorphic genome with extensive expansion of environment-responsive genes, and plasticity is positively correlated with local adaptation (*10*, *22*). In this study, we produced a chromosome-level assembly of the estuarine oyster genome, re-sequenced 264 wild oysters collected from 11 estuaries, and conducted transcriptomic studies of environmental response to understand its genetic variation, population structure, phenotypic plasticity and genomic signatures of selection or bottleneck that may be linked to environmental changes. Our results show that the estuarine oyster has significantly lower genetic diversity than its sister-species probably due to the impact of past glaciation on its unique estuarine lifestyle. Its population structure is heavily influenced by geological events and ocean currents. Expansion and selection in regulatory regions of environment-responsive genes may enhance phenotypic plasticity that is critical for the adaptation to rapidly changing environments.

Results and Discussion

Genome assembly and annotation. We produced a chromosome-level assembly of the estuarine oyster genome of an estimated size of 583.42 Mb (fig. S1, table S1), using a combination of nanopore long-reads (184 Gb), Illumina paired-end short-reads (64 Gb) and Hi-C (106 Gb) sequences and a hierarchical assembly approach. The final assembly consisted of 630 contigs with a N50 of 6.97 Mb, spanning 613.89 Mb, 99.6% of which or 416 scaffolds with a scaffold N50 of 62.26 Mb were assembled into 10 linkage groups corresponding to the haploid chromosome number (Fig. 1b and c, table S2). To our knowledge, this is the most contiguous assembly produced with nanopore long-read sequencing for a bivalve mollusc (*29-31*). Over 97.9% of genomic short-reads and 97.2% RNA-seq reads were mapped to the assembly that also captured 92.54% of the Benchmarking Universal Single Copy Orthologs (BUSCO) datasets (Fig. 1d, table S3), indicating the assembly has a high level of completeness. The accuracy of genome sequence was 98.32% as compared with Sanger sequencing (table S4). These results indicate that the estuarine oyster genome assembly is of high quality and can be used for down-stream analyses.

The estuarine oyster genome encoded 29,631 protein-coding genes as indicated by homology, *de novo* prediction and mRNA transcripts, and 96.13% of which were functionally annotated (table S5). Various non-coding RNA sequences were also identified and annotated in the genome, including 1,077 transfer RNAs, 20 microRNAs and 131 ribosomal RNAs. A total of 332.40 Mb (54.14%) of repetitive elements were identified (table S6), which is higher than the 43% observed in the Pacific oyster (*32*). Gene density was inversely correlated to the repetitive element content across all chromosomes (fig. S2, ρ = -0.308, p < 0.001). Genome-wide polymorphism was 0.58%, which is less than half as that of the Pacific oyster (*22*), probably due to population bottleneck caused by past glaciations more severely impacting its estuarine lifestyle (see below).

Genome resequencing, variation calling and population structure. We generated

3.81 Tb clean whole-genome resequencing data from 264 wild oysters collected from 11 estuaries covering most of the distribution range (*26, 27*) (Fig. 2a). The genome mapping rate averaged 95.3% varied from 86.5% to 96.7%, and the mapped read depth averaged 19.89×. The data generated 145,271,754 SNPs (ranging from 487,881 to 640,962 per individual) and 103,080,822 indels (ranging from 342,486 to 443,381 per individual). Overall, there were 0.47 heterozygous SNPs per Kb per individual (table S7), which was ~35-fold lower than that in Pacific oyster populations (*10*).

Structure analysis of genome-wide SNPs revealed significant differentiation among different geographic populations, consistent with previously analyses of fitness-related traits, neutral markers and transcriptomic data (*26, 33-35*), but with higher resolution. The optimal number of population clusters was identified as $k = 3$ (fig. S3), representing three main regions along the coast of northern China (NC, 5 sites), middle China (MC, 2 sites) and southern China (SC, 4 sites) (fig. S4). Principle component analysis (PCA), explaining 16% of genetic variance by two PCs, consistently revealed three distinct populations corresponding to NC, MC and SC. Further, fine-scale subpopulations were detected where oysters from Qingdao (QD) and southern subpopulation (SC-b) including Taishan (TS) and Qinzhou (QZh) were separated from NC and SC, respectively (Fig. 2b). Moreover, phylogenetic analysis using neighbor-joining (NJ) method supported PCA clustering, by first distinguishing southern populations from others and then identified another subpopulation (NC-a) within NC located in estuaries of southern Bohai Sea including Binzhou (BZ) and Dongying (DY) (Fig. 2c). A total of six subpopulations were identified for 11 estuaries, greatly improving the resolution of the fine-population structure. Pairwise F_{ST} using all polymorphic positions revealed exceptionally high divergence between SC and other populations, ranged from 0.143 to 0.225 (Fig. 2d), while divergence within SC, MC and NC populations was much lower (table S8). Oysters from MC and NC were clustered together in phylogenetic tree with a lower genetic divergence ($F_{ST} < 0.05$), which is comparable with the divergence among populations of the Pacific oyster in north China (*10*). Linkage disequilibrium (LD, measured as r^2) decreased to

half of its maximum value around 2.54 - 3.00 kb in the three populations (fig. S5), which is substantially slower than the LD decay in the Pacific oyster (~0.1 kb) (*10*). These results provide unprecedented insights into the fine-scale population structure of the estuarine oyster. The finding of exceptionally low sequence diversity, slow LD decay and high population divergence in the estuarine oyster compared with the Pacific oyster suggests that the two species experienced different evolutionary forces.

Historical glaciation, geological events and oceanographic forces shaping diversity and distribution. Population structure of the estuarine oyster was largely concordant with the direction of ocean currents during the summer, where the northern or southern coastal currents are not crossed except over middle populations near the Yangtze River estuary (Fig. 2a and fig. S6). Nucleotide diversity (π) was highest in middle populations (3.56×10^{-4}) and QD oysters (3.59×10^{-4}), likely because converging southern and northern currents bring increased genetic diversity to the middle populations (Fig. 3a). These findings indicate that ocean currents play important role in shaping and maintaining population structure of the estuarine oyster (*10, 36*). The exceptionally high divergence between SC and NC populations can be explained by the fact that currents from the south and north do not cross over and cannot facilitate gene flow. Freshwater discharge from Yangtze River is considered as a major barrier limiting gene flow between north and south populations of marine organisms (*8, 37-40*). For the estuarine oyster, however, populations on the north (NT) and south (SH) side of Yangtze River were clustered together as MC, indicating Yangtze River is not a barrier to gene flow for the estuarine oyster that thrives in low salinity water of estuaries.

To reconstruct the demographic history, Pairwise Sequentially Markovian Coalescent (PSMC) method were used to assess fluctuations in effective population size (*Ne*) in response to Quaternary climatic change using genome data of two or three estuarine oysters from each of the three populations, as well as three previously sequenced Pacific oysters as comparison (*10*). Both of species were severely affected by

glaciation events during the past million year as their *Ne* peaked at ~0.90 mya before the Mindel glaciation (MG, 0.68~0.80 mya) and then was substantially decreased over three periods of glaciation including MG, Riss glaciation (RG, 0.24~0.37 mya) and Würm glaciation (WG, 10,000~120,000 years ago). The *Ne* of both species reached their bottom during the last glaciation WG, but Pacific oyster populations rebounded early and to higher levels than the estuarine oyster, suggesting the last ice age had a greater impact on the estuarine oyster. Also, during the interglacial period before the last glaciation at ~0.2 mya, the SC and NC populations of the estuarine oyster started to diverge (Fig. 3b). We also estimated divergence time between SC and NC based on cytochrome oxidase I (COI) sequence data (*29*) using divergence time between *C. gigas* and *C. angulata* as reference (*39, 41*). The COI-based estimate placed the divergence time at 0.14~0.63 mya, which is close to the 0.2 mya estimated by PSMC with whole-genome data (Fig. 3b). The divergence time coincided with the formation land bridge between Taiwan and mainland China from 0.2 mya to 25,000 years ago by tectonic movement (*42*), creating a physical barrier to gene flow between southern and northern populations that is now maintained by ocean currents.

The nucleotide diversity of all three populations of estuarine oyster was 25-fold lower than that of the Pacific oyster ($\pi_{_C.\ gigas} = 9.27 \times 10^{-3}$, Fig. 3c). Similarly, stickleback fishes adapted to freshwater areas exhibited lower π and *Ne* values than counterparts dwelling in brackish areas (*43*). These findings suggest that climate change may affect species with different lifestyles differently and the estuarine oyster may be more sensitive to climate change than the Pacific oyster that inhabits more open waters of high salinity. Further, *Ne* curves of middle and northern populations split ~90,000 years ago, which corresponded to the great sea level fall at the sub-glaciation of WG when Bohai Sea dried up (*44*). The lower *Ne* and nucleotide diversity of northern population (Fig. 3a, b) support that a stronger bottleneck occurred in estuarine oysters of Bohai Sea. Relatively lower nucleotide diversity was also found in Bohai populations of the Pacific oyster, possibly due to the same sea level fall (*10*). The role of bottlenecks and geographic isolation resulting from historical glaciations and

tectonic events in shaping phylogeography has been demonstrated in other molluscs, such as the divergence between Atlantic coast and Gulf of Mexico populations of the eastern oyster *Crassostrea virginica* (*7*). Our results provide putative divergence times among estuarine oyster populations linked to historical events and suggest past climate and tectonic movement played an important role in shaping genetic diversity and population differentiation in the estuarine oyster.

To explore the effects of selection and genetic drift, we compared highly heterozygous SNPs in northern and southern populations. The number of SNPs that are highly heterozygous in NC only (14,373) were 1.89-fold higher than those highly heterozygous in SC only (7,595) across 10 chromosomes (Fig. 3d). Both directional selection and genetic bottleneck can decrease the number of heterozygous SNPs. The finding that southern oysters had significantly higher ratio of genes with non-synonymous SNPs (35.67% ± 0.35%) than the middle (33.33% ± 0.22%) and northern (31.82% ± 0.29%) oysters ($p < 0.01$, Fig. 3e), suggests that the southern oysters experienced stronger selection. Stronger selection, potentially from strong environmental disturbance, decreased the numbers of heterozygous SNPs in southern oysters. Thus, in addition to isolation and bottlenecks from historical glaciation, geological events and oceanographic forces, selection or local adaptation may also play an important role in shaping variation and phylogeography of the estuarine oyster.

Signatures of selection. Oysters inhabiting northern and southern estuaries experience significantly different environmental conditions. Southern habitats are characterized by high temperature and low salinity. Satellite remote sensing data from 2000 to 2017 indicated that the monthly average sea surface temperature (SST) of southern habitats was 10.35 □ higher than that of northern habitats (fig. S7). Salinity at the northern BZ site was 10.98 ‰ higher than the southern TS site (*3*). Climate change may enhance the difference and cause salinity to increase at north habitats but decrease at south habitats (*45, 46*). Thus, temperature and salinity are the two most

important environmental factors driving adaptive divergence between northern and southern populations. With discontinuous distribution and limited gene flow, the southern population became locally adapted and evolved higher tolerance to high temperature and low salinity (*3*). We expect that some genomic regions were subjected to selection and contributed to adaptation to higher temperature and lower salinity conditions in the southern population.

To identify signatures of selection sweeps, we calculated the fixation index (F_{ST}) and selection statistics (Tajima's *D*) between two population pairs (SC vs. NC and SC vs. MC) and identified F_{ST} outliers (top 1%, $F_{ST_north\ vs.\ south}$ >= 0.693, $F_{ST_middle\ vs.\ south}$ >= 0.637). Only genomic regions surrounding selective peaks that overlapped between the two population pairs and located at the valleys of Tajima's *D* values in one of the three populations were considered as under selection. A total of 24 selective regions spanning 51 candidate genes (44 annotated) were identified along chromosomes 2, 3, 4, 6, 8 and 9 among three oyster populations (Fig. 4a, b and fig. S8-13, table S9). Most of these candidate genes are involved in response to environmental disturbances in salinity and temperature (*47-54*).

To assess transcriptomic response of the estuarine oyster to temperature and salinity disturbances, we conducted RNA-seq analysis of oysters exposed to elevated temperature (6 hours under 37 □) and high salinity (7 days under 60 ‰). Only genes with 10 or more aligned reads in >90% samples were used for subsequent analyses. About 44.17% (10,279 of 23,270) and 11.7% (2,757 of 23,650) of genes were differentially expressed under high salinity and temperature stresses, respectively, with 1,088 genes responsive to both stressors (fig. S14). For the 51 candidate genes from regions under selection, a total of 29 genes were expressed, and 75.9% (22 of 29) and 58.6% (17 of 29) of which were differentially expressed under high salinity and high temperature, respectively ($p < 0.05$, Fig. 4c), indicating most genes under selection are involved in response to environmental disturbances in these two factors. Thirteen genes responded to both thermal and salinity stresses, while only three genes were not sensitive to the two stressors. Nine and four genes highly responsive to high

salinity and high temperature, respectively. The finding that most of genes from regions under selection are involved in response to temperature and salinity disturbances suggest that these two environmental factors are important drivers of adaptive evolution in the estuarine oyster.

Expansion of genes contributing to temperature and salinity adaptation. Among the 24 regions under selection, we found two clusters of tandemly duplicated genes belonging to *solute carrier* families, 10 copies of *Slc23a2* and four copies of *monocarboxylate transporter 12* (*Mct12*, also known as *Slc16a12*) (fig. S13c), located in the two regions of chromosome 9 with high divergence (F_{ST} = 0.81 and 0.76) among the three oyster populations (fig. S13d). The genomic region spanning *Slc23a2* gene families exhibited extremely low Tajima's *D* values in northern oysters, while these spanning *Mct12* gene families had extremely low Tajima's *D* values in southern oysters (fig. S13e). These findings indicate that *Slc23a2* and *Mct12* genes were under directional selection in northern and southern environments respectively, highlighting the critical role of *Slc* family genes in adaptation of marine species, as also reported in porpoises and coral (*47, 55-57*), to salinity and temperature variations.

The ten copies of *Slc23a2* family belong to three orthogroups, where two of them are annotated as purine permease (a: OG0011985 and c: OG0000489) and the other is annotated as uric acid transporter (OG0000633). Four copies of *Mct12* gene family belong to one orthogroup annotated as purine efflux pump (OG0000571). All these orthogroups were extensively expanded in the estuarine oyster, as well as in other two other oyster species (*Crassostrea virginica* and *Crassostrea hongkongensis*) that occur in warm and low-salinity estuarine environments, but not so in *C. gigas* that inhabit cool, open and high-salinity waters (fig. S15). Three copies of *Slc23a2* (*Slc23a2_a1*, *Slc23a2_a2* and *Slc23a2_c2*) in two expanded orthogroups responded to both temperature and salinity challenges, while three copies of *Mct12* (*Mct12_1*, *Mct12_2* and *Mct12_3*) responded to salinity challenge (Fig. 4c). The expansion of these environment-responsive genes may enhance transcriptional complexity or plasticity

and play an important role in adaption to diverse temperature and salinity conditions in the estuarine oyster and two other species inhabiting similar environments. This finding provides further evidence that gene duplication is critical for stress adaptation, as previously demonstrated for the expansion of *heat shock protein* and *inhibitor of apoptosis* gene families in the Pacific oyster and other marine bivalves (*22, 31, 58*).

Stronger selection in upstream regulatory regions of environment-responsive genes with high plasticity. To understand the interaction between divergence and plasticity, we examined divergence in different genomic regions (genic, upstream and downstream) with F_{ST} and transcriptional plasticity of the 29 genes from regions under selection in response to environmental translocations. F_1 progeny produced from northern and southern populations were acclimatized at both northern and southern habitats for three months before transcriptional analysis. Fourteen of the 29 genes exhibited higher plasticity (HP) where they showed significantly differentiated expression when translocated to nonnative environments in both oyster populations ($p < 0.05$), while other genes had lower plasticity (LP) and their expression didn't strongly respond to environmental translocation/change (Fig. 5a). The transcriptional plasticity of the HP genes was 19.15% higher than that of LP genes ($p = 0.0255$, fig. S16).

For the whole genome, genic regions showed significantly higher F_{ST} values (mean $F_{ST_genic} = 0.163$) than that of intergenic regions ($F_{ST_intergenic} = 0.138$, $p < 0.001$, Wilcoxon signed-rank tests, Fig. 5b), indicating stronger selection in genic regions driving differentiation between northern and southern populations. For all 29 genes from regions under selection, both genic ($F_{ST} = 0.7745$) and intergenic ($F_{ST} = 0.7585$) regions showed strong selection signals or divergence compared with all genes in the genome, and the difference between genic and intergenic regions was not significant ($p > 0.05$). For both genic and intergenic regions, genes with high plasticity showed significantly ($p = 0.0230$) higher divergence ($F_{ST} = 0.7816$) between northern and southern oysters than LP genes ($F_{ST} = 0.7274$) (Fig. 5b). Specifically, the upstream

intergenic regions of HP genes exhibited significantly (p = 0.01512) higher divergence (F_{ST} = 0.7958) between northern and southern populations than that of LP genes (F_{ST} = 0.7402), while there was no significant difference between the two type of genes for genic and downstream intergenic regions ($p > 0.05$, Fig. 5c). Further, LP genes showed higher divergence in genic regions. While selection preferentially targeted genic regions at genome level and for LP genes, HP genes showing high plasticity exhibited stronger selection in upstream intergenic regions, where critical regulatory elements such as promoter and enhancers reside, potentially regulate gene expression and enhance transcriptional plasticity (*19*). These results suggest that selection and divergence in upstream regulatory regions may enhance phenotypic plasticity that contributes to the survival and adaption of organisms facing environmental disturbances. The mechanism of selection favoring plasticity is not clear at this time. Directional selection tends to reduce genetic variation and facilitate local adaptation. Selection acting on regulatory elements may create divergence and transcriptional complexity that enhance phenotypic plasticity (*18*, *19*) at species level. Directional selection acting on duplicated genes can potentially direct duplicated member genes to express under different conditions and therefore enhance overall phenotypic plasticity. It is also possible that balancing selection retains diversity in regulatory elements and increase plasticity. It has been suggested that balancing selection is pervasive in oysters and important for their evolution (*59*).

In conclusion, analysis of the estuarine oyster genome revealed exceptionally low genetic diversity and fine-scale population structures, which were shaped and maintained by climate history, geological events and oceanographic forces. Integration of genomic and transcriptomic analyses revealed genes in regions under selection are mostly involved in environmental response including the expanded *solute carrier* gene families that are important for environmental adaptation. Expansion and selection in upstream regulatory regions of environment-responsive genes may enhance transcriptional complexity and phenotypic plasticity that are critical for the adaptation to rapidly changing environments.

Materials and Methods

Genome sequencing. A wild adult estuarine oyster *Crassostrea ariakensis* was obtained from Binzhou, Bohai Sea, northern China. Four tissue samples (gill, mantle, adductor muscle and labial palp) were collected and flash-frozen in liquid nitrogen. Genomic DNA was extracted from the adductor muscle and used to construct libraries for Oxford Nanopore Technologies' long-read sequencing. In addition, libraries with insert size of ~350 bp were prepared and sequenced using Illumina HiSeq 4000 platform.

Genome size and heterozygosity. Trimmed Illumina short reads were used to generate the k-mer copy number (KCN) distribution. We selected 21-mer for KCN distribution which showed two distinct peaks (fig. S1). The first peak (KCN = 45) represents heterozygous single copy k-mers while the second peak (KCN = 90) represents homozygous single copy k-mers in the genome. Genome size was estimated by the formula G = K_num/peak depth.

Contig-level assembly using long-reads. Nanopore long reads, with a read N50 of 33,230 and a mean read length of 23,240 bp, were used for initial genome assembly. Error correction of clean data was conducted using Canu (*60*) v1.5, and then were assembled using Canu, WTDBG2 (*61*) and SMARTdenovo tools. Quickmerge (*62*) v0.2.2 was used to join the three assemblies, and the assembly was corrected for 3 cycles using long reads by Racon (*63*) and for 3 cycles using Illumina reads by Pilon (*64*) v1.22 with default parameters. The initial assembly of the estuarine oyster genome was 613,892,480 bp in length with a contig N50 of 6,967,240 bp.

Chromosome-level assembly with Hi-C. The same genomic DNA extracted from the adductor muscle was used to construct Hi-C library for with the Illumina HiSeq 4000 platform. Contigs and scaffolds which were then sorted and oriented into super scaffolds using LACHESIS (*65*) with the following parameters: cluster_min_re_sites

= 47, cluster_max_link_density = 2, cluster_noninformative_ratio = 2, order_min_n_res_in_trun = 40, order_min_n_res_in_shreds = 41.

Genome evaluation. Hi-C contact heatmap of the number of Hi-C links between 100 kb windows on the pseudochromosomes was used to assess the accuracy of the Hi-C assembly. Benchmarking Universal Single-Copy Orthologs (BUSCO) v3.0.2 with 978 conserved genes were used to assess the completeness and accuracy of gene coverage. The completeness and accuracy of the assembly was also evaluated by mapping rate of RNA-seq reads (see **Protein coding gene annotation**) and Illumina genomic reads with Burrows-Wheeler Aligner (*66*) v.0.7.8.

Repeat annotation. Transposable elements (TEs) were identified and classified using homology and *de novo*-based approaches. RepeatScout and LTR_FINDER were used to construct *de novo* repeat libraries. The *de novo*-based libraries were further classified with PASTEClassifier (*67*) to obtain a consensus library, and combined with the repeat library of Repbase data. RepeatMasker (*68*) v4.0.5 was used to identify TEs in the estuarine oyster genome with the combined library.

Protein-coding gene annotation. Protein-coding genes were identified with three methods: *de novo* prediction, homology-based prediction and RNA-seq-based prediction. For *de novo* prediction, five *ab initio* gene prediction programs, Genscan (*69*) v1.0, Augustus (*70*) v2.4, GlimmerHMM (*71*) v3.0.4, GeneID (*72*) v1.4 and SNAP(*73*), were used to predict genes in the repeat-masked genome. For homolog-based prediction, protein sequences from 10 well-annotated species, including *Homo sapiens*, *Danio rerio*, *Aplysia californica*, *Strongylocentrotus purpuratus*, *C. gigas*, *C. virginica*, *Biomphalaria glabrata*, *Lingula anatina*, *Octopus bimaculoides* and *Mizuhopecten yessoensis*, were downloaded from GenBank and aligned to the repeat-masked estuarine oyster genome using tblastn (*74*) with E-value ≤ 1E-05. We used GeMoMa (*75*) v1.3.1 to predict gene models based on alignment

sequences. For RNA-seq-based prediction, RNA-seq data generated from four tissues (gill, mantle, adductor muscle and labial palp) using ONT long-read sequencing platform were filtered to remove adaptors and then trimmed to remove low-quality bases. Clean reads were aligned to reference genome using TopHat2 (*76*) and then assembled using Trinity (*77*). Full transcriptome-based genome annotation was predicted using PASA (*78*) v2.2.2. Finally, EVidenceModeler (*79*) (EVM) v1.1.1 was used to generate a weighted and non-redundant gene set by integrating all gene models predicted by the three methods.

Homologous sequences in the genome were identified with genBlastA (*80*) v1.0.4 using the integrated gene set, and GeneWise (*81*) was used to identify pseudogenes. Transfer RNAs (tRNAs) were defined using tRNAscan-SE (*82*) v1.3.1 software with eukaryote default parameters. MicroRNA and rRNA were identified with Infernal BLASTN (*83*) against the Rfam (*84*) database v12.0.

Functional annotation of protein-coding genes was conducted by aligning them to the NCBI non-redundant protein (*85*) (NR), SwissProt (*86*), KOG (*87*) and TrEMBL (*86*) databases using BLAST (*83*) v2.2.31 with a maximal e-value of 1e-05. Domains were identified by searching against Pfam (*88*) database using HMMER (*89*) v3.0. Genes were mapped to Gene Ontology (GO) terms and KEGG pathways to identify their best functional classification.

Whole-genome resequencing and mapping. We collected 264 wild estuarine oysters from 11 estuaries (Fig. 3a), covering most of its distribution range (*26*, *27*). Genomic DNA was isolated from gill tissue with standard phenol-chloroform extraction and used to construct paired-end libraries with an insert size of ~350 bp according to the manufacturer's instructions (Illumina Inc., San Diego, CA, USA) for sequencing on the Illumina HiSeq X Ten Sequencer. We obtained ~14.42 Gb of clean data for each sample, giving an average depth of 19.9X coverage (15-28X) (table S8). The 150-bp paired-end reads were mapped to the estuarine oyster reference genome (PRJNA715058) with the BWA (*66*) using default parameters (bwa mem –M -t 10 -T

20). Mapping data were then converted into the BAM format and sorted by SAMtools v.1.3.1 (*90*) to remove duplicate reads. Read pairs with the highest mapping quality were retained if multiple pairs have identical external coordinates.

Variant calling and annotation. The Genome Analysis Toolkit (GATK) v.3.7 (*91*) module HaplotypeCaller was used to obtain high-quality variation calling of each sample. SNPs were further filtered with parameters 'QD<2.0 || FS>60.0 || MQ<40.0'. Similarly, indels were called and filtered using parameters 'QD<2.0 || FS>60.0'. Filtered SNPs were annotated by SnpEff (*92*) and then classified into regions of exon, intron, splicing site, and upstream and downstream intergenic regions, and as heterozygous or homozygous variants. To characterize the types of variants in northern and southern oysters, Plink (*93*) was used to filter raw SNPs using parameters of MAF > 0.05 and Int > 0.8. The retained SNPs were singly classified as highly heterozygous in a population if more than half individuals were heterozygous in that population but not in the other population. Variations in exons were further categorized as synonymous or non-synonymous SNPs. Two-sided two-sample Wilcoxon signed-rank tests were conducted to test whether the ratios of genes with nonsynonymous mutations were different between northern and southern populations, using the function *wilcoxsign-test* in R package "coin".

Population analysis. Population structure was inferred using ADMIXTURE v.1.23 (*94*) with default settings. The number of assumed genetic clusters *K* ranged from 2 to 5, and the optimum *K* was assessed with cross-validation errors. The individual-based neighbor-joining (NJ) phylogenetic tree was constructed using MEGA (*95*) under Kimura 2-Parameter model with 1000 bootstraps, and visualized using FigTree. PCA was performed with whole-genome SNPs of all 264 individuals using Eigensoft (*96*). To evaluate LD decay, parameter r^2 between any two loci was calculated within each chromosome using Plink v.1.07 (*93*) with the command –ld-window-r2 0 –ld-window 99999 –ld-window-kb 500. The average r^2 values were calculated for each length of

distance and the genome-wide LD was averaged across all chromosomes. The LD decay was plotted against the length of distance. Popgenome R package (*97*) was used to calculate Tajima's *D*, global F_{ST} and nucleotide diversity (*p*) using a 100-kb sliding window with the step size of 10-kb.

Demographic history. We implemented PSMC (*98*) to estimate dynamics of effective population size (*Ne*) and possible divergence time over the past several million years. A total of eight estuarine oysters from northern (n = 3), middle (n = 2) and southern (n = 3) populations and three Pacific oysters (*10*) with high sequencing depth (20 - 28×) were used. To minimize the probability of false positives, sequencing depth of SNPs was filtered with parameters: MinDepth = average depth/3, MaxDepth = average depth×2. The PSMC parameters were set as: -N25 -t15 -r5 -p '4 + 25*2 + 4 + 6' to estimate historical *Ne*. The estimated generation time (*g*) was set as 1 for both species, while mutation rates (μ) were calculated, following the formula $T_{_divergence} = Ks/2\mu$, as 0.3×10^{-8} and 0.2×10^{-8} for estuarine and Pacific oysters, respectively.

Selection signature detection. To identify selection sweeps potentially contributing to adaptation to southern environments, we calculated fixation (F_{ST}) and selection statistics (Tajima's *D*) between two pairs of populations, north vs. south and middle vs. south, in a 100-kb sliding window with a step size of 10-kb. Genomic regions showing strong selection signals were defined as: 1) regions with top 1% F_{ST} values that overlapped in both pair comparisons; and 2) regions located at valleys of Tajima's *D* values distribution along the chromosome in one of the three populations.

Response to temperature and salinity disturbance. To investigate responses of estuarine oysters to challenges of elevated temperature and high salinity, we collected wild oysters and exposed them to different temperatures (20 □ and 37 □ for 6 hours) and salinities (20 and 60 for 7 days), respectively. Gills from five oysters were individually sampled and flash-frozen in liquid nitrogen for subsequent transcriptomic

analysis.

Reciprocal transplantation experiments. To explore the plasticity of candidate genes from regions under selection, we measured transcriptional changes in oysters subjected to native and non-native environments after reciprocal transplantation (*3*). Briefly, wild oysters derived from northern (Binzhou: BZ, Bohai Sea) and southern (Taishan: TS, East China Sea) environments were collected and used to produce F_1 progeny. For each population, 40 males and 40 females were selected as parents. Eggs were pooled and then divided into 40 beakers, each fertilized with sperm from one of the 40 males to create all possible matings. Zygotes fathered by every eight males were combined and cultured as one group, and the five groups were reared in separate tanks in the hatchery and nursery to juvenile stage. Two-month-old F_1 juveniles from each of the two populations were outplanted at two source habitats to assess their responses to reciprocal transplantation or environmental change. After three months of acclimation at northern and southern environments, gills of five oysters were sampled from each of population at both habitats *in situ* and flash-frozen in liquid nitrogen for subsequent transcriptomic analysis.

Transcriptomic analysis. Total RNA was isolated from gills sampled from laboratory challenge experiment (high temperature and high salinity) and field reciprocal transplantation experiment, using the RNAprep Pure Tissue Kit (Tiangen) following the manufacturer's protocol. The RNA integrity and concentration were examined with 1.2% agarose gel electrophoresis and Nanodrop 2000 spectrophotometer, respectively. DNA contamination was removed with DNAse I treatment. RNA integrity was further assessed using an Agilent Bioanalyzer 2100 and the RNA Nano 6000 Assay Kit. One μg RNA per sample was used to construct sequencing libraries using NEBNext Ultra^{TM} RNA Library Prep Kit for 150-bp paired-end sequencing on an Illumina HiSeq 4000 platform. Clean data were obtained by removing reads containing adapters, reads containing ploy-N and low-quality reads. TopHat2 was

used to map clean reads to the estuarine oyster genome. StringTie v2.0 was used for read assembly. Only reads with perfect match or one mismatch were further analyzed and annotated. Gene expression levels were estimated by fragments per kilobase of transcript per million fragments mapped (FPKM). We used DESeq2 to determine differentially expressed genes (DEGs) between different populations or treatments. Genes with an adjusted p-value < 0.01 using the Benjamin and Hochberg's approach were accepted as DEGs. For genes from regions under selection, those significantly differentially expressed between northern and southern habitats in both oyster populations were defined as high plasticity genes (HP), while others were defined as low plasticity genes (LP). A hierarchical cluster analysis was performed to show differential expression of these genes, using the *pheatmap* package in R software.

Supplementary materials

Supplementary material for this article is available at the end of this file.

References and Notes

1. O. Hoegh-Guldberg, J. F. Bruno, The impact of climate change on the world's marine ecosystems. *Science* **328**, 1523-1528 (2010).
2. C. Chou, J. C. H. Chiang, C.-W. Lan, C.-H. Chung, Y.-C. Liao, C.-J. Lee, Increase in the range between wet and dry season precipitation. *Nature Geoscience* **6**, 263-267 (2013).
3. A. Li, C. Wang, W. Wang, Z. Zhang, M. Liu, Z. She, Z. Jia, G. Zhang, L. Li, Molecular and Fitness Data Reveal Local Adaptation of Southern and Northern Estuarine Oysters (Crassostrea ariakensis). *Frontiers in Marine Science* **7**, (2020).
4. R. F. Schneider, A. Meyer, How plasticity, genetic assimilation and cryptic genetic

554 variation may contribute to adaptive radiations. *Molecular ecology* **26**, 330-350 (2017).

555 5. E. Crispo, The Baldwin effect and genetic assimilation: revisiting two mechanisms of
556 evolutionary change mediated by phenotypic plasticity. *Evolution* **61**, 2469-2479
557 (2007).

558 6. D. W. Pfennig, M. A. Wund, E. C. Snell-Rood, T. Cruickshank, C. D. Schlichting, A. P.
559 Moczek, Phenotypic plasticity's impacts on diversification and speciation. *Trends in*
560 *ecology & evolution* **25**, 459-467 (2010).

561 7. N. E. Buroker, W. K. Hershberger, K. K. Chew, Population Genetics of the Family
562 Ostreidae. II. Interspecific Studies of the Genera *Crassostrea* and *Saccostrea*. *Marine*
563 *Biology* **54**, 171-184 (1979).

564 8. G. Ni, E. Kern, Y. W. Dong, Q. Li, J. K. Park, More than meets the eye: The barrier
565 effect of the Yangtze River outflow. *Molecular ecology* **26**, 4591-4602 (2017).

566 9. Y. Xiao, D. Ma, M. Dai, Q. Liu, Z. Xiao, J. Li, J. Liu, S. Xu, Q. Cheng, The impact of
567 Yangtze River discharge on the genetic structure of a population of the rock
568 bream,Oplegnathus fasciatus. *Marine Biology Research* **12**, 426-434 (2016).

569 10. L. Li, A. Li, K. Song, J. Meng, X. Guo, S. Li, C. Li, P. De Wit, H. Que, F. Wu, W. Wang,
570 H. Qi, F. Xu, R. Cong, B. Huang, Y. Li, T. Wang, X. Tang, S. Liu, B. Li, R. Shi, Y. Liu, C.
571 Bu, C. Zhang, W. He, S. Zhao, H. Li, S. Zhang, L. Zhang, G. Zhang, Divergence and
572 plasticity shape adaptive potential of the Pacific oyster. *Nat Ecol Evol* **2**, 1751-1760
573 (2018).

574 11. C. D. Kenkel, M. V. Matz, Gene expression plasticity as a mechanism of coral
575 adaptation to a variable environment. *Nature Ecology & Evolution* **1**, 0014 (2016).

576 12. T. Armarego-Marriott, Climatic selection and gene expression plasticity. *Nature*
577 *Climate Change* **11**, 4-4 (2021).
578 13. C. A. Vargas, N. A. Lagos, M. A. Lardies, C. Duarte, P. H. Manriquez, V. M. Aguilera,
579 B. Broitman, S. Widdicombe, S. Dupont, Species-specific responses to ocean
580 acidification should account for local adaptation and adaptive plasticity. *Nature*
581 *Ecology & Evolution* **1**, 84 (2017).
582 14. L. Y. Yampolsky, T. M. Schaer, D. Ebert, Adaptive phenotypic plasticity and local
583 adaptation for temperature tolerance in freshwater zooplankton. *Proceedings.*
584 *Biological sciences / The Royal Society* **281**, 20132744 (2014).
585 15. J. Sandoval-Castillo, K. Gates, C. J. Brauer, S. Smith, L. Bernatchez, L. B.
586 Beheregaray, Adaptation of plasticity to projected maximum temperatures and across
587 climatically defined bioregions. *Proceedings of the National Academy of Sciences* **117**,
588 17112-17121 (2020).
589 16. D. W. Whitman, A. A. Agrawal, *What is phenotypic plasticity and why is it important?*
590 (Phenotypic Plasticity of Insects, Science Publishers, 2009).
591 17. L. E. Eierman, M. P. Hare, Reef-Specific Patterns of Gene Expression Plasticity in
592 Eastern Oysters (Crassostrea virginica). *The Journal of heredity* **107**, 90-100 (2016).
593 18. M. Kelly, Adaptation to climate change through genetic accommodation and
594 assimilation of plastic phenotypes. *Philosophical Transactions of the Royal Society B:*
595 *Biological Sciences* **374**, 20180176 (2019).
596 19. V. Grishkevich, I. Yanai, The genomic determinants of genotype x environment
597 interactions in gene expression. *Trends in genetics : TIG* **29**, 479-487 (2013).

598 20. A. Li, L. Li, K. Song, W. Wang, G. Zhang, Temperature, energy metabolism, and
599 adaptive divergence in two oyster subspecies. *Ecology and evolution* **7**, 6151-6162
600 (2017).
601 21. P.-A. Gagnaire, J.-B. Lamy, F. Cornette, S. Heurtebise, L. Degremont, E. Flahauw, P.
602 Boudry, N. Bierne, S. Lape`gue, Analysis of Genome-Wide Differentiation between
603 Native and Introduced Populations of the Cupped Oysters *Crassostrea gigas* and
604 *Crassostrea angulata*. *Genome biology and evolution* **10**, 2518-2534 (2018).
605 22. G. Zhang, X. Fang, X. Guo, L. Li, R. Luo, F. Xu, P. Yang, L. Zhang, X. Wang, H. Qi, Z.
606 Xiong, H. Que, Y. Xie, P. W. Holland, J. Paps, Y. Zhu, F. Wu, Y. Chen, J. Wang, C.
607 Peng, J. Meng, L. Yang, J. Liu, B. Wen, N. Zhang, Z. Huang, Q. Zhu, Y. Feng, A.
608 Mount, D. Hedgecock, Z. Xu, Y. Liu, T. Domazet-Loso, Y. Du, X. Sun, S. Zhang, B. Liu,
609 P. Cheng, X. Jiang, J. Li, D. Fan, W. Wang, W. Fu, T. Wang, B. Wang, J. Zhang, Z.
610 Peng, Y. Li, N. Li, J. Wang, M. Chen, Y. He, F. Tan, X. Song, Q. Zheng, R. Huang, H.
611 Yang, X. Du, L. Chen, M. Yang, P. M. Gaffney, S. Wang, L. Luo, Z. She, Y. Ming, W.
612 Huang, S. Zhang, B. Huang, Y. Zhang, T. Qu, P. Ni, G. Miao, J. Wang, Q. Wang, C. E.
613 Steinberg, H. Wang, N. Li, L. Qian, G. Zhang, Y. Li, H. Yang, X. Liu, J. Wang, Y. Yin, J.
614 Wang, The oyster genome reveals stress adaptation and complexity of shell formation.
615 *Nature* **490**, 49-54 (2012).
616 23. A. Li, L. Li, W. Wang, G. Zhang, Evolutionary trade-offs between baseline and plastic
617 gene expression in two congeneric oyster species. *Biology Letters* **15**, 20190202
618 (2019).
619 24. M. W. Beck, R. D. Brumbaugh, L. Airoldi, A. Carranza, L. D. Coen, C. Crawford, O.

620 Defeo, G. J. Edgar, B. Hancock, M. C. Kay, H. S. Lenihan, M. W. Luckenbach, C. L.
621 Toropova, G. Zhang, X. Guo, Oyster Reefs at Risk and Recommendations for
622 Conservation, Restoration, and Management. *BioScience* **61**, 107-116 (2011).
623 25. X. Guo, S. E. Ford, Infectious diseases of marine molluscs and host responses as
624 revealed by genomic tools. *Philosophical transactions of the Royal Society of London.*
625 *Series B, Biological sciences* **371**, (2016).
626 26. H. Wang, X. Guo, G. Zhang, F. Zhang, Classification of jinjiang oysters Crassostrea
627 rivularis (Gould, 1861) from China, based on morphology and phylogenetic analysis.
628 *Aquaculture* **242**, 137-155 (2004).
629 27. M. F. Zhou, S. K. Allen, A review of published work on *Crassostrea ariakensis*. *Journal*
630 *of Shellfish Research* **22**, 1-20 (2003).
631 28. H. Wang, L. Qian, G. Zhang, X. Liu, A. Wang, Y. Shi, N. Jiao, X. Guo, Distribution of
632 *Crassostrea ariakensis* in China. *Journal of Shellfish Research* **25**, 789-790 (2006).
633 29. C. M. Bai, L. S. Xin, U. Rosani, B. Wu, Q. C. Wang, X. K. Duan, Z. H. Liu, C. M. Wang,
634 Chromosomal-level assembly of the blood clam, Scapharca (Anadara) broughtonii,
635 using long sequence reads and Hi-C. *GigaScience* **8**, (2019).
636 30. J. Peng, Q. Li, L. Xu, P. Wei, P. He, X. Zhang, L. Zhang, J. Guan, X. Zhang, Y. Lin, J.
637 Gui, X. Chen, Chromosome-level analysis of the Crassostrea hongkongensis genome
638 reveals extensive duplication of immune-related genes in bivalves. *Molecular ecology*
639 *resources* **20**, 980-994 (2020).
640 31. H. Song, X. Guo, L. Sun, Q. Wang, F. Han, H. Wang, G. A. Wray, P. Davidson, Q.
641 Wang, Z. Hu, C. Zhou, Z. Yu, M. Yang, J. Feng, P. Shi, Y. Zhou, L. Zhang, T. Zhang,

642 The hard clam genome reveals massive expansion and diversification of inhibitors of
643 apoptosis in Bivalvia. *BMC Biol* **19**, 15 (2021).
644 32. C. Penaloza, A. Gutierrez, L. Eory, S. Wang, X. Guo, A. Archibald, T. Bean, R.
645 Houston, A chromosome-level genome assembly for the Pacific oyster Crassostrea
646 gigas. *GigaScience* **10**, (2021).
647 33. J. Xiao, J. F. Cordes, H. Wang, X. Guo, K. S. Reece, Population genetics of
648 Crassostrea ariakensis in Asia inferred from microsatellite markers. *Marine Biology*
649 **157**, 1767-1781 (2010).
650 34. W.-J. Kim, S. T. Dammannagoda, H. Jung, I. S. Baek, H. S. Yoon, S. D. Choi,
651 Mitochondrial DNA sequence analysis from multiple gene fragments reveals genetic
652 heterogeneity of Crassostrea ariakensis in East Asia. *Genes Genom.* **36**, 611-624
653 (2014).
654 35. X. Liu, L. Li, A. Li, Y. Li, W. Wang, G. Zhang, Transcriptome and Gene Coexpression
655 Network Analyses of Two Wild Populations Provides Insight into the High-Salinity
656 Adaptation Mechanisms of Crassostrea ariakensis. *Marine biotechnology* **21**, 596-612
657 (2019).
658 36. C. Li, M. Olave, Y. Hou, G. Qin, R. F. Schneider, Z. Gao, X. Tu, X. Wang, F. Qi, A.
659 Nater, A. F. Kautt, S. Wan, Y. Zhang, Y. Liu, H. Zhang, B. Zhang, H. Zhang, M. Qu, S.
660 Liu, Z. Chen, J. Zhong, H. Zhang, L. Meng, K. Wang, J. Yin, L. Huang, B. Venkatesh,
661 A. Meyer, X. Lu, Q. Lin, Genome sequences reveal global dispersal routes and
662 suggest convergent genetic adaptations in seahorse evolution. *Nature*
663 *communications* **12**, 1094 (2021).

664 37. Y. Dong, H. Wang, G. Han, C. Ke, X. Zhan, T. Nakano, G. A. Williams, The Impact of
665 Yangtze River Discharge, Ocean Currents and Historical Events on the Biogeographic
666 Pattern of *Cellana toreuma* along the China Coast. *PloS ONE* **7**, e36178 (2012).
667 38. G. Ni, Q. Li, L. Kong, X. D. Zheng, Phylogeography of bivalve *Cyclina sinensis*: testing
668 the historical glaciations and Changjiang River outflow hypotheses in northwestern
669 Pacific. *PLoS ONE* **7**, e49487 (2012).
670 39. H. Wang, L. Qian, X. Liu, G. Zhang, X. Guo, Classification of a common cupped oyster
671 from southern China. *Journal of Shellfish Research* **29**, 857-866 (2010).
672 40. H. Wang, G. Zhang, X. Liu, X. Guo, Classification of Common Oysters from North
673 China. *Journal of Shellfish Research* **27**, 495-503 (2008).
674 41. J. Ren, X. Liu, F. Jiang, X. Guo, B. Liu, Unusual conservation of mitochondrial gene
675 order in *Crassostrea* oysters: evidence for recent speciation in Asia. *BMC evolutionary*
676 *biology* **10**, 394 (2010).
677 42. M. Kimura, Paleogeography of the Ryukyu Islands. *Tropics* **10**, 5-24 (2000).
678 43. J. A. M. Raeymaekers, A. Chaturvedi, P. I. Hablutzel, I. Verdonck, B. Hellemans, G. E.
679 Maes, L. De Meester, F. A. M. Volckaert, Adaptive and non-adaptive divergence in a
680 common landscape. *Nature communications* **8**, 267 (2017).
681 44. Y. Qin, Y. Zhao, S. Zhao, *Geology of the Bohai Sea* (Science Press, Beijing, 1985).
682 45. N. Skliris, R. Marsh, S. A. Josey, S. A. Good, C. Liu, R. P. Allan, Salinity changes in
683 the World Ocean since 1950 in relation to changing surface freshwater fluxes. *Climate*
684 *Dynamics* **43**, 709-736 (2014).
685 46. M. M. Mekonnen, A. Y. Hoekstra, Four billion people facing severe water scarcity.

686 *Science Advances* **2**, e1500323 (2016).

687 47. X. Zhou, X. Guang, D. Sun, S. Xu, M. Li, I. Seim, W. Jie, L. Yang, Q. Zhu, J. Xu, Q.
688 Gao, A. Kaya, Q. Dou, B. Chen, W. Ren, S. Li, K. Zhou, V. N. Gladyshev, R. Nielsen,
689 X. Fang, G. Yang, Population genomics of finless porpoises reveal an incipient
690 cetacean species adapted to freshwater. *Nature communications* **9**, 1276 (2018).

691 48. C. A. Ribeiro, F. Balestro, V. Grando, M. Wajner, Isovaleric acid reduces Na+,
692 K+-ATPase activity in synaptic membranes from cerebral cortex of young rats. *Cellular*
693 *and molecular neurobiology* **27**, 529-540 (2007).

694 49. Y. Huang, J. Niwa, G. Sobue, G. E. Breitwieser, Calcium-sensing receptor
695 ubiquitination and degradation mediated by the E3 ubiquitin ligase dorfin. *The Journal*
696 *of biological chemistry* **281**, 11610-11617 (2006).

697 50. H. Vienken, N. Mabrouki, K. Grabau, R. F. Claas, A. Rudowski, N. Schomel, J.
698 Pfeilschifter, D. Lutjohann, G. van Echten-Deckert, D. Meyer Zu Heringdorf,
699 Characterization of cholesterol homeostasis in sphingosine-1-phosphate
700 lyase-deficient fibroblasts reveals a Niemann-Pick disease type C-like phenotype with
701 enhanced lysosomal Ca(2+) storage. *Scientific reports* **7**, 43575 (2017).

702 51. M. Pagano, M. A. Clynes, N. Masada, A. Ciruela, L.-J. Ayling, S. Wachten, D. M. F.
703 Cooper, Insights into the residence in lipid rafts of adenylyl cyclase AC8 and its
704 regulation by capacitative calcium entry. *Am J Physiol Cell Physiol* **296**, C607–C619
705 (2009).

706 52. E. J. Weinman, W. P. Dubinsky, S. Shenolikar, Reconstitution of cAMP-Dependent
707 Protein Kinase Regulated Renal Na^+-H^+ Exchanger. *J. Membr. Biol.* **101**, 11-18

708 (1988).

709 53. M. C. Fonteles, R. N. Greenberg, H. S. A. Monteiro, M. G. Currie, L. R. Forte,
710 Natriuretic and kaliuretic activities of guanylin and uroguanylin in the isolated perfused
711 rat kidney. *The American Journal of Physiology* **F191-F197**, (1998).

712 54. D. B. Stern, C. E. Lee, Evolutionary origins of genomic adaptations in an invasive
713 copepod. *Nat Ecol Evol* **4**, 1084-1094 (2020).

714 55. A. M. Barrio, S. Lamichhaney, G. Fan, N. Rafati, M. Pettersson, H. Zhang, J. Dainat, D.
715 Ekman, M. Hoppner, P. Jern, M. Martin, B. Nystedt, X. Liu, W. Chen, X. Liang, C. Shi,
716 Y. Fu, K. Ma, X. Zhan, C. Feng, U. Gustafson, C.-J. Rubin, M. S. Almen, M. C. Martina
717 Blass10, A. Folkvord, L. Laikre, N. Ryman, S. M.-Y. Lee, X. Xu, L. Andersson, The
718 genetic basis for ecological adaptation of the Atlantic herring revealed by genome
719 sequencing. *eLife* **5**, e12081 (2016).

720 56. C. D. Kenkel, E. Meyer, M. V. Matz, Gene expression under chronic heat stress in
721 populations of the mustard hill coral (*Porites astreoides*) from different thermal
722 environments. *Molecular ecology* **22**, 4322-4334 (2013).

723 57. P. J. Hoglund, K. J. Nordstrom, H. B. Schioth, R. Fredriksson, The solute carrier
724 families have a remarkably long evolutionary history with the majority of the human
725 families present before divergence of Bilaterian species. *Mol Biol Evol* **28**, 1531-1541
726 (2011).

727 58. X. Guo, Y. He, L. Zhang, C. Lelong, A. Jouaux, Immune and stress responses in
728 oysters with insights on adaptation. *Fish & shellfish immunology* **46**, 107-119 (2015).

729 59. X. Guo, C. Li, H. Wang, Z. Xu, Diversity and Evolution of Living Oysters. *Journal of*

730 *Shellfish Research* **37**, 755-771 (2018).

731 60. S. Koren, B. P. Walenz, K. Berlin, J. R. Miller, N. H. Bergman, A. M. Phillippy, Canu:
732 scalable and accurate long-read assembly via adaptive k-mer weighting and repeat
733 separation. *Genome research* **27**, 722-736 (2017).

734 61. V. Jayakumar, Y. Sakakibara, Comprehensive evaluation of non-hybrid genome
735 assembly tools for third-generation PacBio long-read sequence data. *Briefings in*
736 *bioinformatics* **20**, 866-876 (2019).

737 62. M. Chakraborty, J. G. Baldwin-Brown, A. D. Long, J. J. Emerson, Contiguous and
738 accurate de novo assembly of metazoan genomes with modest long read coverage.
739 *Nucleic acids research* **44**, e147 (2016).

740 63. R. Vaser, I. Sovic, N. Nagarajan, M. Sikic, Fast and accurate de novo genome
741 assembly from long uncorrected reads. *Genome research* **27**, 737-746 (2017).

742 64. B. J. Walker, T. Abeel, T. Shea, M. Priest, A. Abouelliel, S. Sakthikumar, C. A. Cuomo,
743 Q. Zeng, J. Wortman, S. K. Young, A. M. Earl, Pilon: An Integrated Tool for
744 Comprehensive Microbial Variant Detection and Genome Assembly Improvement.
745 *PLoS ONE* **9**, e112963 (2014).

746 65. J. N. Burton, A. Adey, R. P. Patwardhan, R. Qiu, J. O. Kitzman, J. Shendure,
747 Chromosome-scale scaffolding of de novo genome assemblies based on chromatin
748 interactions. *Nature biotechnology* **31**, 1119-1125 (2013).

749 66. H. Li, R. Durbin, Fast and accurate short read alignment with Burrows-Wheeler
750 transform. *Bioinformatics* **25**, 1754-1760 (2009).

751 67. C. Hoede, S. Arnoux, M. Moisset, T. V. Chaumier, O. Inizan, V. Jamilloux, H.

752 Quesneville, PASTEC: An Automatic Transposable Element Classification Tool. *PLoS*
753 *ONE* **9**, e91929 (2014).
754 68. M. Tarailo-Graovac, N. Chen, Using RepeatMasker to identify repetitive elements in
755 genomic sequences. *Curr Protoc Bioinformatics* **Chapter 4**, Unit 4 10 (2009).
756 69. C. Burge, S. Karlin, Prediction of complete gene structures in human genomic DNA.
757 *Journal of molecular biology* **268**, 78-94 (1997).
758 70. M. Stanke, S. Waack, Gene prediction with a hidden Markov model and a new intron
759 submodel. *Bioinformatics* **19 Suppl 2**, ii215-225 (2003).
760 71. W. H. Majoros, M. Pertea, S. L. Salzberg, TigrScan and GlimmerHMM: two open
761 source ab initio eukaryotic gene-finders. *Bioinformatics* **20**, 2878-2879 (2004).
762 72. T. Alioto, E. Blanco, G. Parra, R. Guigo, Using geneid to Identify Genes. *Curr Protoc*
763 *Bioinformatics* **64**, e56 (2018).
764 73. I. Korf, Gene finding in novel genomes. *Bmc Bioinformatics* **5**, 59 (2004).
765 74. S. F. Altschul, T. L. Madden, A. A. Schäffer, J. Zhang, Z. Zhang, W. Miller, D. J.
766 Lipman, Gapped BLAST and PSI-BLAST: a new generation of protein database
767 search programs. *Nucleic acids research* **25**, 3389-3402 (1997).
768 75. J. Keilwagen, F. Hartung, M. Paulini, S. O. Twardziok, J. Grau, Combining RNA-seq
769 data and homology-based gene prediction for plants, animals and fungi. *Bmc*
770 *Bioinformatics* **19**, 189 (2018).
771 76. D. Kim, G. Pertea, C. Trapnell, H. Pimentel, R. Kelley, S. L. Salzberg, TopHat2:
772 accurate alignment of transcriptomes in the presence of insertions, deletions and gene
773 fusions. *Genome biology* **14**, R36 (2013).

774 77. M. G. Grabherr, B. J. Haas, M. Yassour, J. Z. Levin, D. A. Thompson, I. Amit, X.
775 Adiconis, L. Fan, R. Raychowdhury, Q. Zeng, Z. Chen, E. Mauceli, N. Hacohen, A.
776 Gnirke, N. Rhind, F. di Palma, B. W. Birren, C. Nusbaum, K. Lindblad-Toh, N.
777 Friedman, A. Regev, Full-length transcriptome assembly from RNA-Seq data without
778 a reference genome. *Nature biotechnology* **29**, 644-652 (2011).
779 78. M. A. Campbell, B. J. Haas, J. P. Hamilton, S. M. Mount, C. R. Buell, Comprehensive
780 analysis of alternative splicing in rice and comparative analyses with Arabidopsis.
781 *BMC genomics* **7**, 327 (2006).
782 79. B. J. Haas, S. L. Salzberg, W. Zhu, M. Pertea, J. E. Allen, J. Orvis, O. White, C. R.
783 Buell, J. R. Wortman, Automated eukaryotic gene structure annotation using
784 EVidenceModeler and the Program to Assemble Spliced Alignments. *Genome biology*
785 **9**, R7 (2008).
786 80. R. She, J. S. Chu, K. Wang, J. Pei, N. Chen, GenBlastA: enabling BLAST to identify
787 homologous gene sequences. *Genome research* **19**, 143-149 (2009).
788 81. E. Birney, M. Clamp, R. Durbin, GeneWise and Genomewise. *Genome research* **14**,
789 (2004).
790 82. T. M. Lowe, S. R. Eddy, tRNAscan-SE: a program for improved detection of transfer
791 RNA genes in genomic sequence. *Nucleic acids research* **25**, 955-964 (1997).
792 83. S. F. Altschul, W. Gish, W. Miller, E. W. Myers, D. J. Lipman, Basic Local Alignment
793 Search Tool. *Journal of molecular biology* **215**, 403-410 (1990).
794 84. S. Griffiths-Jones, S. Moxon, M. Marshall, A. Khanna, S. R. Eddy, A. Bateman, Rfam:
795 annotating non-coding RNAs in complete genomes. *Nucleic acids research* **33**,

796 D121-124 (2005).

797 85. A. Marchler-Bauer, S. Lu, J. B. Anderson, F. Chitsaz, M. K. Derbyshire, C.
798 DeWeese-Scott, J. H. Fong, L. Y. Geer, R. C. Geer, N. R. Gonzales, M. Gwadz, D. I.
799 Hurwitz, J. D. Jackson, Z. Ke, C. J. Lanczycki, F. Lu, G. H. Marchler, M. Mullokandov,
800 M. V. Omelchenko, C. L. Robertson, J. S. Song, N. Thanki, R. A. Yamashita, D. Zhang,
801 N. Zhang, C. Zheng, S. H. Bryant, CDD: a Conserved Domain Database for the
802 functional annotation of proteins. *Nucleic acids research* **39**, D225-229 (2011).

803 86. B. Boeckmann, A. Bairoch, R. Apweiler, M. C. Blatter, A. Estreicher, E. Gasteiger, M. J.
804 Martin, K. Michoud, C. O'Donovan, I. Phan, S. Pilbout, M. Schneider, The
805 SWISS-PROT protein knowledgebase and its supplement TrEMBL in 2003. *Nucleic*
806 *acids research* **31**, 365-370 (2003).

807 87. R. L. Tatusov, D. A. Natale, I. V. Garkavtsev, T. A. Tatusova, U. T. Shankavaram, B. S.
808 Rao, B. Kiryutin, M. Y. Galperin, N. D. Fedorova, E. V. Koonin, The COG database:
809 new developments in phylogenetic classification of proteins from complete genomes.
810 *Nucleic acids research* **29**, 22-28 (2001).

811 88. R. D. Finn, J. Mistry, B. Schuster-Bockler, S. Griffiths-Jones, V. Hollich, T. Lassmann,
812 S. Moxon, M. Marshall, A. Khanna, R. Durbin, S. R. Eddy, E. L. Sonnhammer, A.
813 Bateman, Pfam: clans, web tools and services. *Nucleic acids research* **34**, D247-251
814 (2006).

815 89. J. Mistry, R. D. Finn, S. R. Eddy, A. Bateman, M. Punta, Challenges in homology
816 search: HMMER3 and convergent evolution of coiled-coil regions. *Nucleic acids*
817 *research* **41**, e121 (2013).

818 90. H. Li, B. Handsaker, A. Wysoker, T. Fennell, J. Ruan, N. Homer, G. Marth, G.
819 Abecasis, R. Durbin, S. Genome Project Data Processing, The Sequence
820 Alignment/Map format and SAMtools. *Bioinformatics* **25**, 2078-2079 (2009).
821 91. A. McKenna, M. Hanna, E. Banks, A. Sivachenko, K. Cibulskis, A. Kernytsky, K.
822 Garimella, D. Altshuler, S. Gabriel, M. Daly, M. A. DePristo, The Genome Analysis
823 Toolkit: a MapReduce framework for analyzing next-generation DNA sequencing data.
824 *Genome research* **20**, 1297-1303 (2010).
825 92. P. Cingolani, A. Platts, L. Wang le, M. Coon, T. Nguyen, L. Wang, S. J. Land, X. Lu, D.
826 M. Ruden, A program for annotating and predicting the effects of single nucleotide
827 polymorphisms, SnpEff: SNPs in the genome of Drosophila melanogaster strain
828 w1118; iso-2; iso-3. *Fly* **6**, 80-92 (2012).
829 93. S. Purcell, B. Neale, K. Todd-Brown, L. Thomas, M. A. Ferreira, D. Bender, J. Maller,
830 P. Sklar, P. I. de Bakker, M. J. Daly, P. C. Sham, PLINK: a tool set for whole-genome
831 association and population-based linkage analyses. *American journal of human*
832 *genetics* **81**, 559-575 (2007).
833 94. D. H. Alexander, J. Novembre, K. Lange, Fast model-based estimation of ancestry in
834 unrelated individuals. *Genome research* **19**, 1655-1664 (2009).
835 95. S. Kumar, G. Stecher, M. Li, C. Knyaz, K. Tamura, MEGA X: Molecular Evolutionary
836 Genetics Analysis across Computing Platforms. *Mol Biol Evol* **35**, 1547-1549 (2018).
837 96. A. L. Price, N. J. Patterson, R. M. Plenge, M. E. Weinblatt, N. A. Shadick, D. Reich,
838 Principal components analysis corrects for stratification in genome-wide association
839 studies. *Nature genetics* **38**, 904-909 (2006).

840 97. B. Pfeifer, U. Wittelsburger, S. E. Ramos-Onsins, M. J. Lercher, PopGenome: an
841 efficient Swiss army knife for population genomic analyses in R. *Mol Biol Evol* **31**,
842 1929-1936 (2014).
843 98. H. Li, R. Durbin, Inference of human population history from individual whole-genome
844 sequences. *Nature* **475**, 493-496 (2011).
845

Acknowledgments: We thank X. Wang, Z. Jia, Z. She, Y. Zhang, Z. Yu, W. Quan, Z. Zeng and Y. Ning for sample collection, and B. Yin and J. Qi for information on marine currents. **Funding:** L.L. is supported by the National Key R&D Program of China (No. 2018YFD0900304) and the Strategic Priority Research Program of the Chinese Academy of Sciences (No. XDA23050402). A.L. is supported by the Distinguished Young Scientists Research Fund of Key Laboratory of Experimental Marine Biology, Chinese Academy of Sciences (No. KLEMB-DYS04) and by China Postdoctoral Science Foundation (No. 2019TQ0324). A.L. and L.L. are supported by Key Deployment Project of Centre for Ocean Mega-Research of Science, Chinese Academy of Sciences (No. COMS2019Q06). L.L. is also supported by the National Natural Science Foundation of China (No. 31572620) and the Technology and the Modern Agro-industry Technology Research System (No. CARS-49). **Author contributions:** L.L., G.Z. and X.G. conceived the study and participated in final data analysis, interpretation and manuscript writing. A.L. carried out data analysis and drafted the manuscript. H.D., A.L., H.C., X.L. and H.Z. contributed to the selective sweep analysis. A.L., Z.Z., K.Z. and C.W. collected and sampled oyster specimens. A.L. and W.W. produced the F_1 progeny. A.L., L.L., X.G. and G.Z. revised the manuscript. All authors approved the manuscript for publication. **Competing interests:** The authors declare no competing interests. **Data and materials availability:** The genome, whole-genome re-sequencing and transcriptome datasets were deposited in the Sequence Read Archive (SRA) database under the accession number PRJNA715058.

Figures

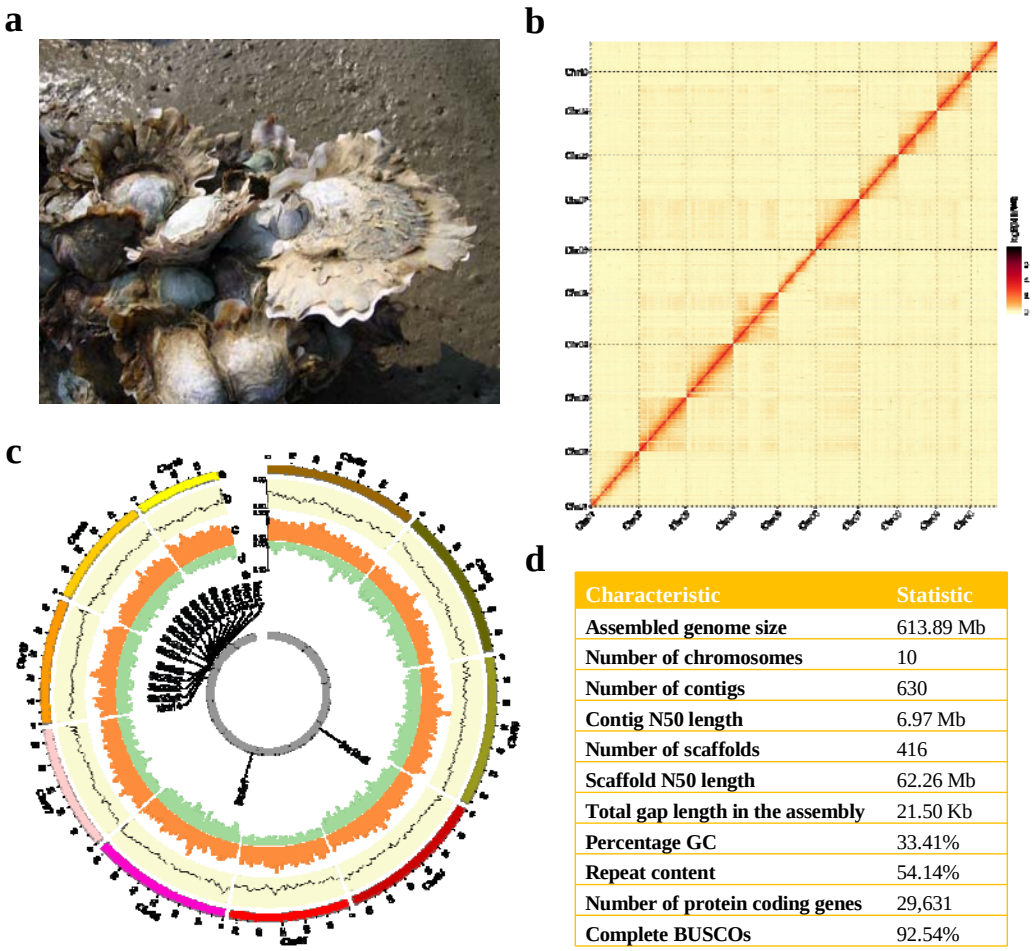

Characteristic	Statistic
Assembled genome size	613.89 Mb
Number of chromosomes	10
Number of contigs	630
Contig N50 length	6.97 Mb
Number of scaffolds	416
Scaffold N50 length	62.26 Mb
Total gap length in the assembly	21.50 Kb
Percentage GC	33.41%
Repeat content	54.14%
Number of protein coding genes	29,631
Complete BUSCOs	92.54%

Fig. 1 | Chromosome-level assembly of the estuarine oyster *Crassostrea ariakensis* genome. **a**, Estuarine oyster (photograph by Lumin Qian). **b**, Hi-C interaction heatmap showing 10 chromosomes of the estuarine oyster. **c**, CIRCOS plot showing 10 chromosomes (a), the distribution of GC content (b), transposable elements (c), coding sequences (d), and duplicated gene cluster of the *solute carrier* families showing selection signals (e, also see **Fig. 4**). **d**, Summary statistics of the genome assembly.

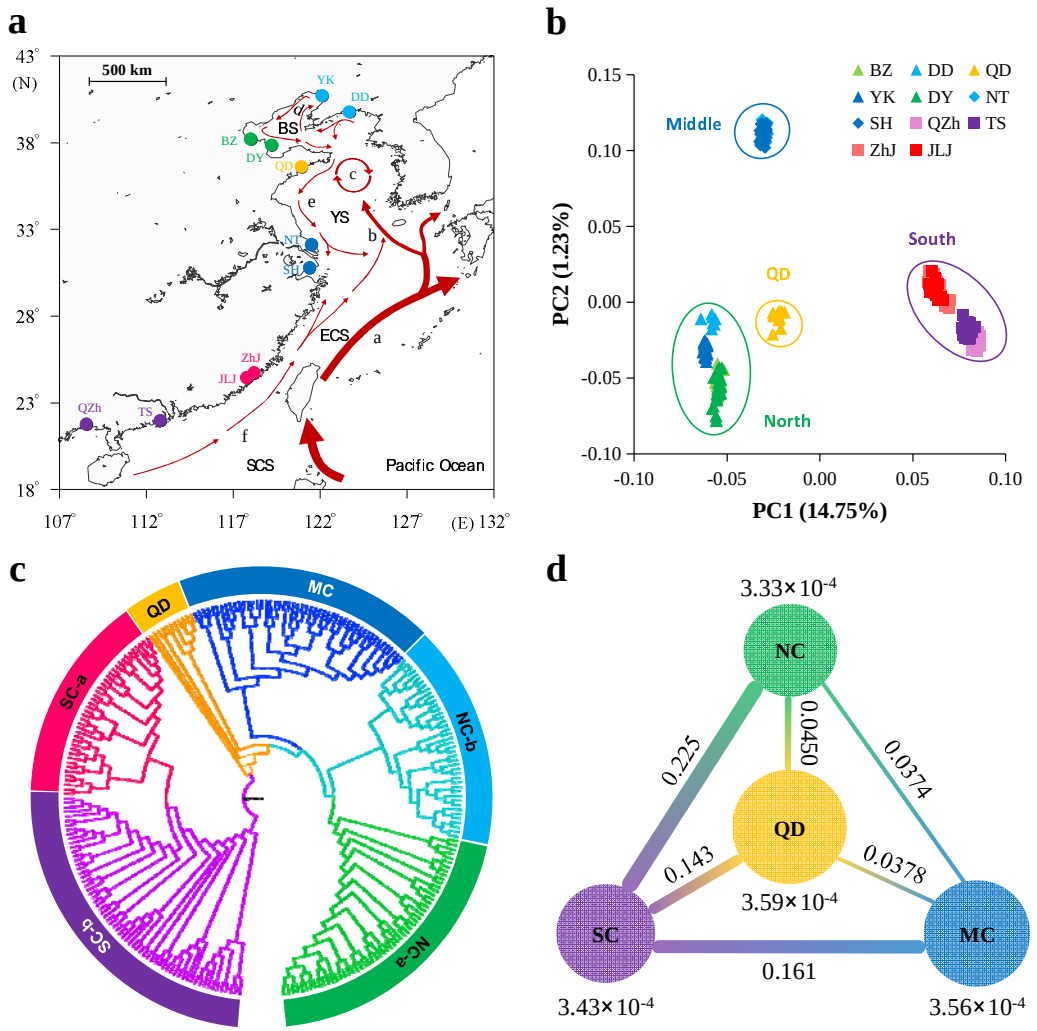

Fig. 2 | Geographic distribution and genetic differentiation of the estuarine oyster populations. a, Sampling locations of 264 resequenced wild oysters from 11 estuaries along the coast of China. The arrowed curves represent ocean currents in summer. a: Kuroshio Current, b: Yellow Sea Warm Current, c: Yellow Sea Cold Water Mass, d: Bohai Sea Circulation, e: China Coastal Current, f: South China Sea Warm Current. SCS: South China Sea, ECS: East China Sea, YS: Yellow Sea, BS: Bohai Sea. DD: Dandong, YK: Yingkou, BZ: Binzhou, DY: Dongying, QD: Qingdao, NT: Nantong, SH: Shanghai, JLJ: Jiulongjiang, ZhJ: Zhangjiang, TS: Taishan, QZh: Qinzhou. **b**, Plots of principal components 1 and 2 of 264 resequenced oysters based on whole-genome data. **c**, Phylogenetic tree of estuarine oysters inferred from genome-wide SNPs by the neighbour-joining (NJ) method. NC-a: northern China, including BZ and DY; NC-b: northern China including DD and YK; MC: middle China including NT and SH; SC-a: southern China including JLJ and ZhJ; and SC-b: southern China including TS and QZh. **d**, Nucleotide diversity (π, under or above the circles) and genetic divergence (F_{ST}, between populations) among four populations.

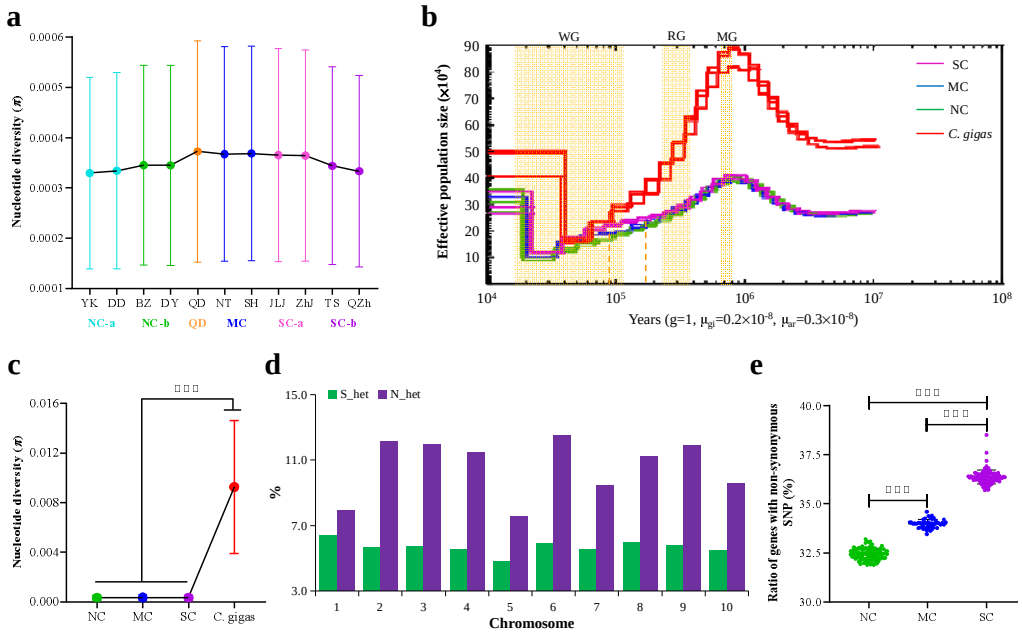

Fig. 3 | Effects of gene flow, historical glaciation and natural selection on diversity and differentiation of the estuarine oyster. a, Nucleotide diversity (π) in 11 geographic populations along the coast of China. **b**, Demographic histories of three populations of the estuarine oyster (ar) (SC, MC and NC), and Pacific oyster (*C. gigas* or gi) inferred by Pairwise Sequentially Markovian Coalescent. Periods of the Mindel glaciation (MG, 0.68~0.80 mya), Riss glaciation (MG, 0.24~0.37 mya) and Würm glaciation (WG, 10,000~120,000 years ago) were shaded by yellow. **c**, Nucleotide diversity (π) of three populations of the estuarine oyster, and Pacific oyster (*C. gigas*). **d**, The ratio of SNPs that are highly heterozygous only in northern (N_het) or only in southern (S_het) populations across 10 chromosomes. **e**, The ratio of genes with non-synonymous SNPs in three oyster populations. Asterisks indicate significant difference (*** $p < 0.001$).

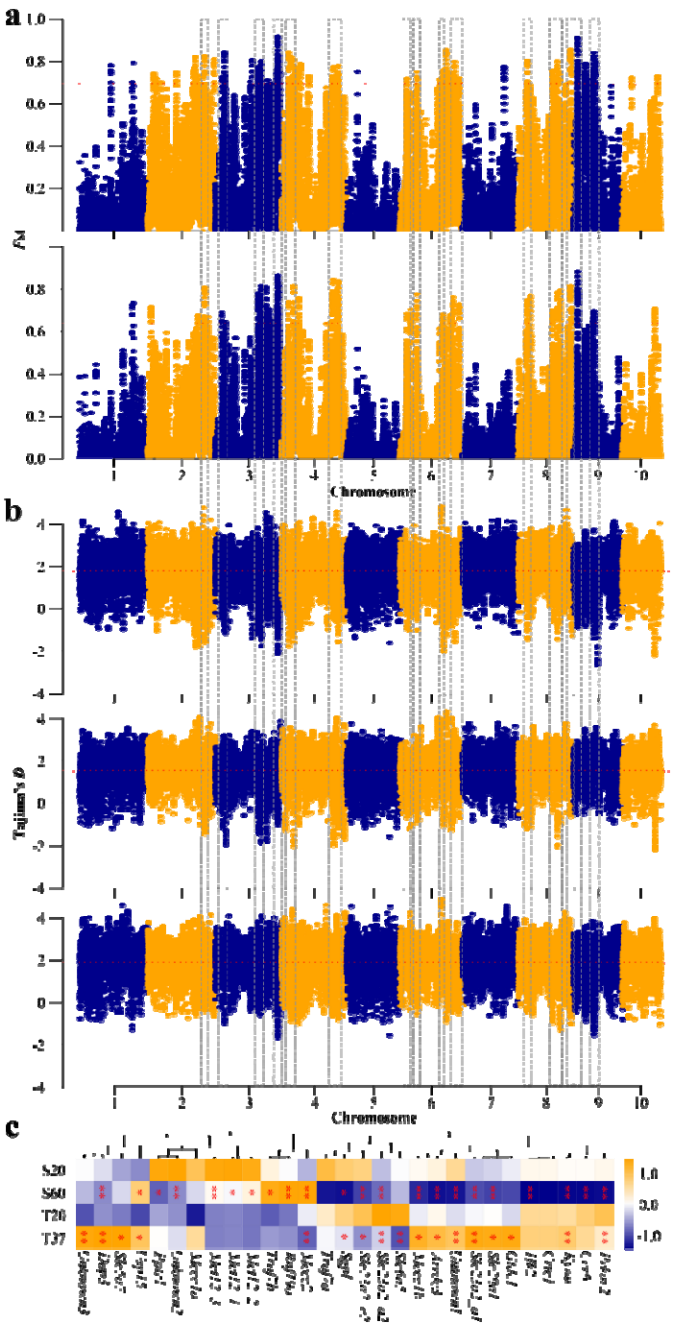

Fig. 4 | Genome-wide distribution of selective sweep signals and transcriptional responses of associated genes to thermal and salinity challenges in the estuarine oyster. a, Global F_{ST} values (top 1%, red lines) between two population pairs: northern vs. southern (up) and middle vs. southern (bottom). **b**, Global Tajima's *D* values in northern (up), middle (middle) and southern (bottom) populations. **c**, Expression of genes under selection exposed to thermal (6 hours at 37 □) and high-salinity (7 days at 60 ‰) challenges. Asterisks indicate significant difference (* $p < 0.05$, ** $p < 0.01$).

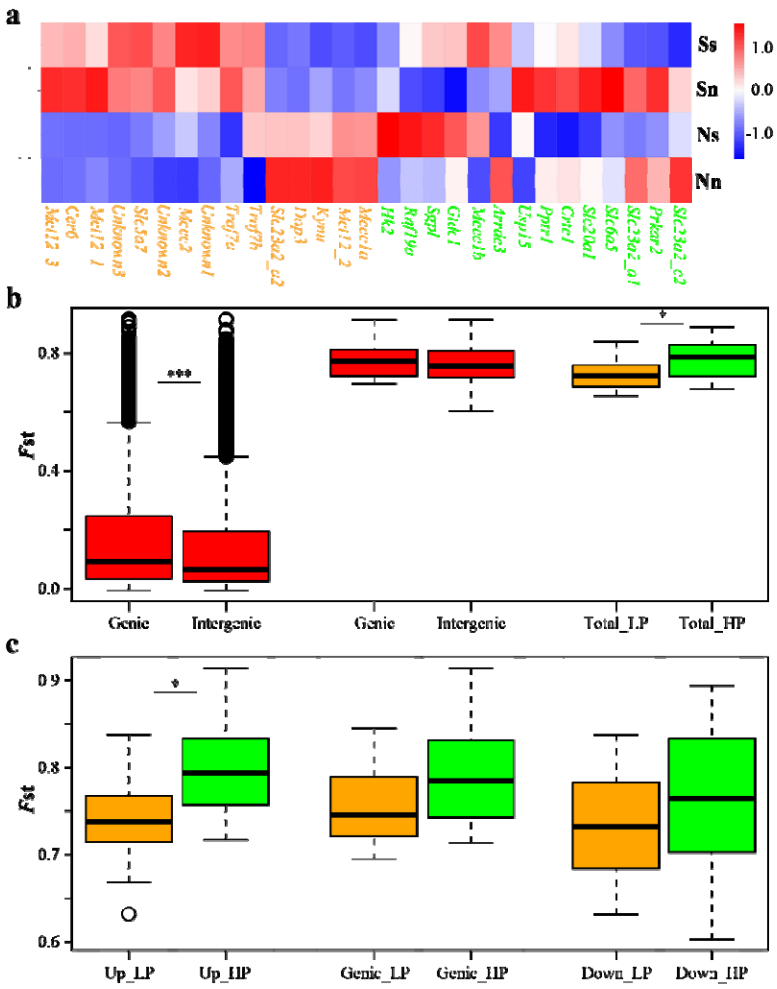

Fig. 5 | Transcriptional and genomic divergence of genes with selection signals in the estuarine oyster. a, Expression level of genes under selection in northern (N) and southern (S) populations (capital letters) acclimated to northern (n) and southern (s) environments (lowercase letters), showing low plasticity (LP, orange) and high plasticity (HP, green) genes. **b**, Genetic divergence (F_{ST}) for genic and intergenic regions at genome level (left) and for 29 genes under selection (middle), and for LP and HP genes in both genic and intergenic regions (Total, right). **c**, Genetic divergence (F_{ST}) for intergenic [Up: upstream (left) and Down: downstream (right)] and genic (middle) regions of LP and HP genes. Asterisks indicate significant difference (* $p < 0.05$, *** $p < 0.001$).

Supplementary Material for

Genome of the estuarine oyster provides insights into climate impact and adaptive plasticity

Subtitle: Insights into climate impact and adaptive plasticity

Ao Li, He Dai, Ximing Guo, Ziyan Zhang, Kexin Zhang, Chaogang Wang, Wei Wang, Hongju Chen, Xumin Li, Hongkun Zheng, Guofan Zhang* and Li Li*

*Corresponding author. Email: lili@qdio.ac.cn and gzhang@qdio.ac.cn

The file includes:
Figs. S1 to S16

Other Supplementary Material for this manuscript includes the following:
Table S1-9

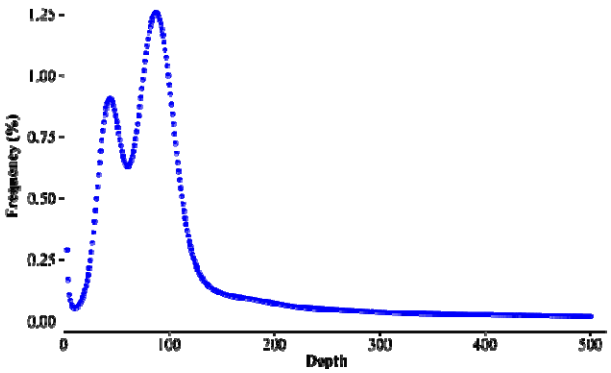

Fig. S1 | Distribution of 21-mer frequency in the sequencing reads used to estimate genome size.

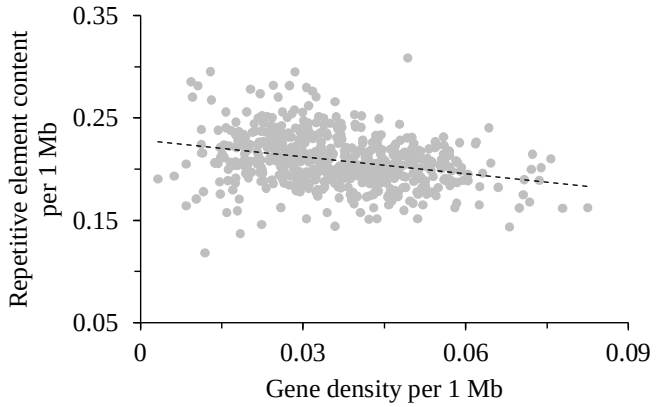

Fig. S2 | Negative correlation between gene density and repetitive element content per 1 Mb across the genome of estuarine oyster.

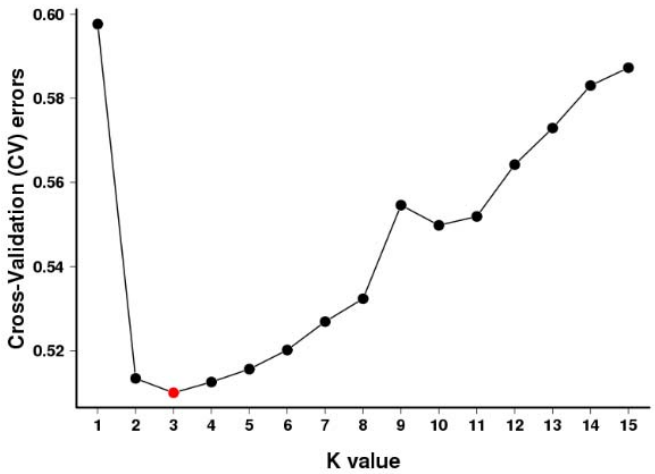

Fig. S3 | Cross-validation error plot for populations of the estuarine oyster.

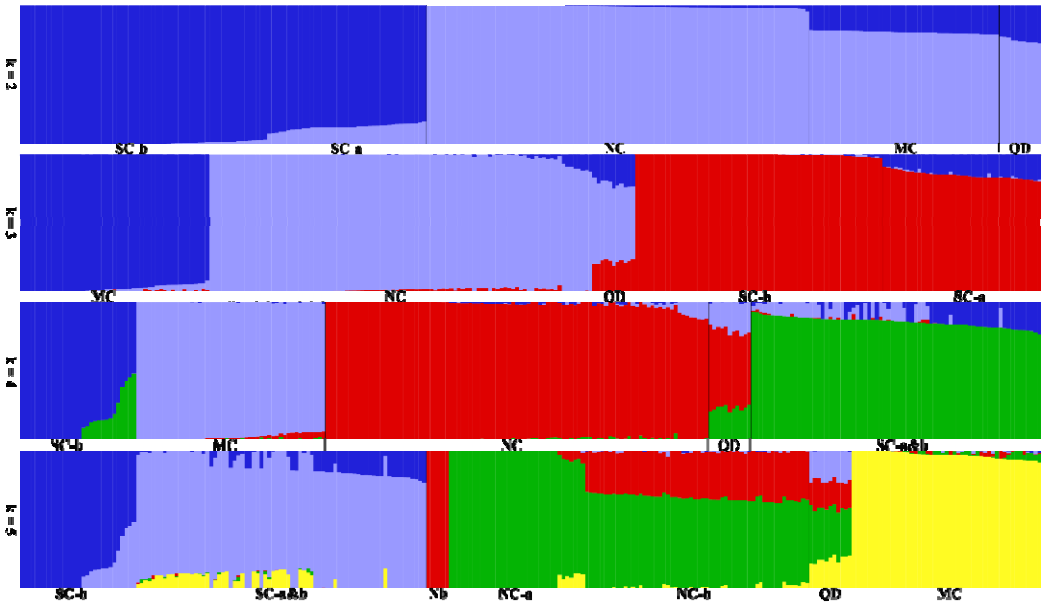

Fig. S4 | Model-based clustering analysis of estuarine oyster populations with ADMIXTURE under different number of groups (K = 2, 3, 4 and 5). SC: southern China. NC: northern China (Nb indicates NC-b). MC: middle China. QD: Qingdao population.

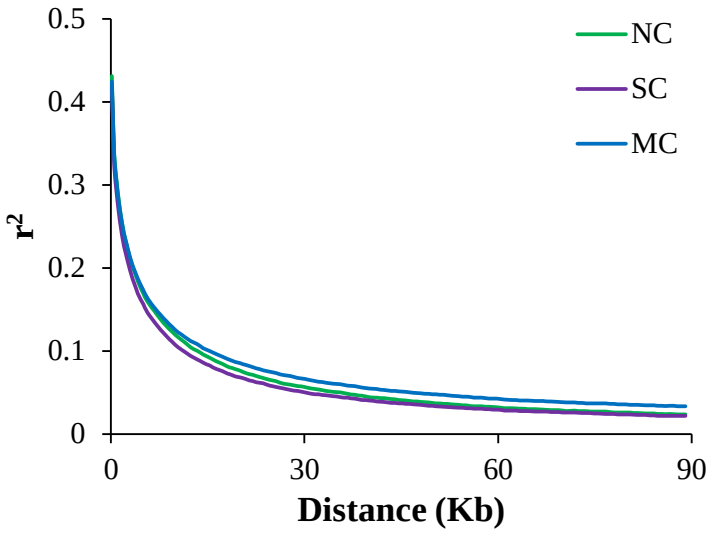

Fig. S5 | Decay of linkage disequilibrium in northern (NC), middle (MC) and southern (SC) populations of the estuarine oyster.

Fig. S6 | Dynamics of average monthly sea surface temperature (SST) and ocean currents along Chinese coastlines. Data for SST and ocean currents were downloaded from MODIS (Jan 2003 to Dec 2019) and OSCAR (Jan 2001 to Dec 2019), respectively.

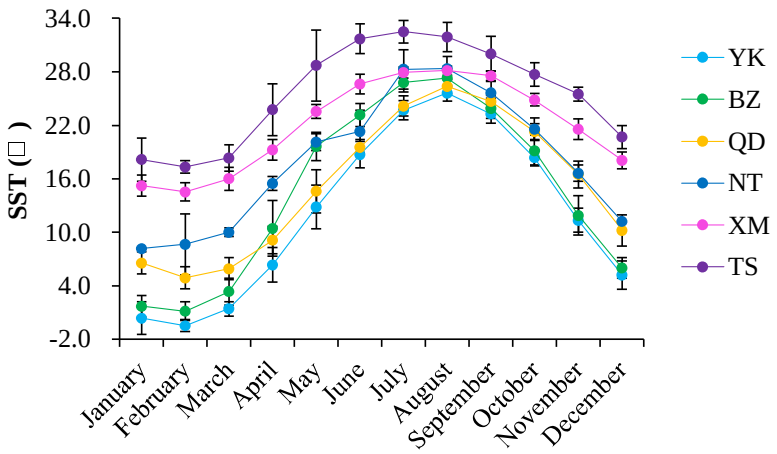

Fig. S7 | Monthly average sea surface temperature (SST) from satellite remote sensing data of six sampling sites from each of six subpopulations during 2000 to 2017.

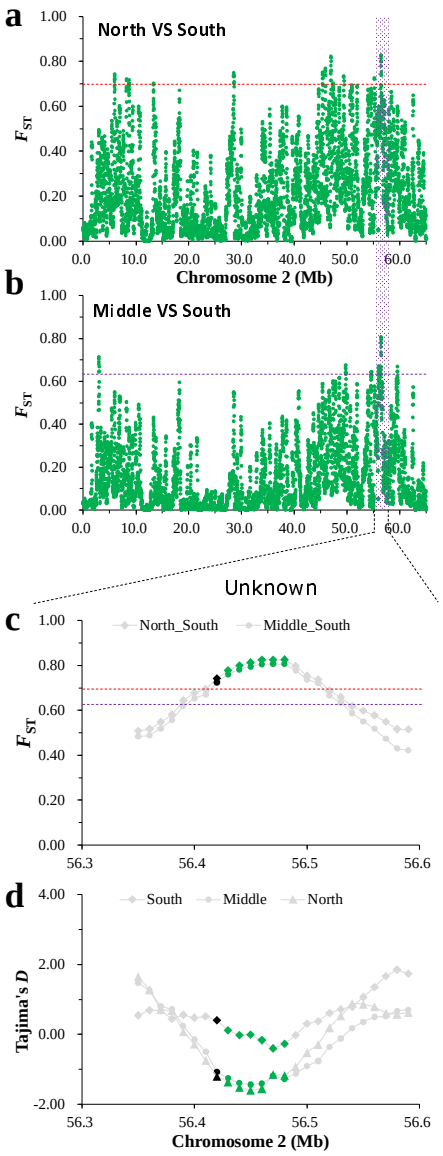

Fig. S8 | Signatures of selection along chromosome 2 in northern, middle and southern populations of the estuarine oyster. a and **b**, Selective sweep signatures identified by top 1% F_{ST} value (dash lines) between northern and southern (**a**), and between middle and southern populations (**b**). **c**, F_{ST} values surrounding selective regions om chromosome 2 between population pairs. **d**, Tajima's *D* surrounding selective regions on chromosome 2 in northern, middle and southern populations of *C. ariakensis*. Noncoding regions were marked with black, and coding regions were green.

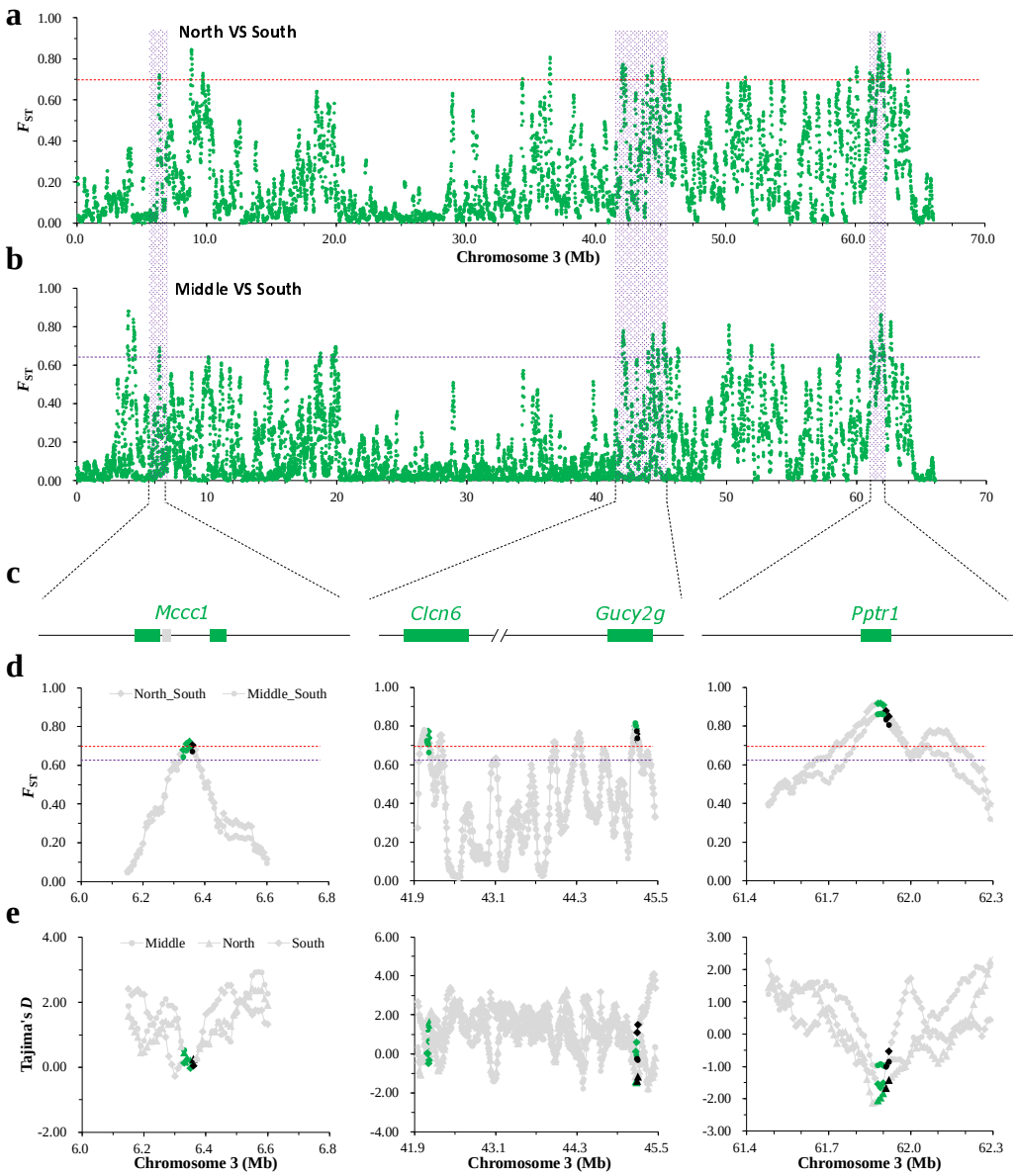

Fig. S9 | Signatures of selection along the chromosome 3 in northern, middle and southern populations of the estuarine oyster. a and **b**, Selective sweep signatures identified by top 1% F_{ST} value (dash lines) between northern and southern (**a**), and between middle and southern populations (**b**). **c**, Models of annotated genes located within selective regions along chromosome 3. **d**, F_{ST} values surrounding selective regions om chromosome 3 between population pairs. **e**, Tajima's *D* surrounding selective regions on chromosome 3 in northern, middle and southern populations. Noncoding regions were marked with black, and coding regions were green.

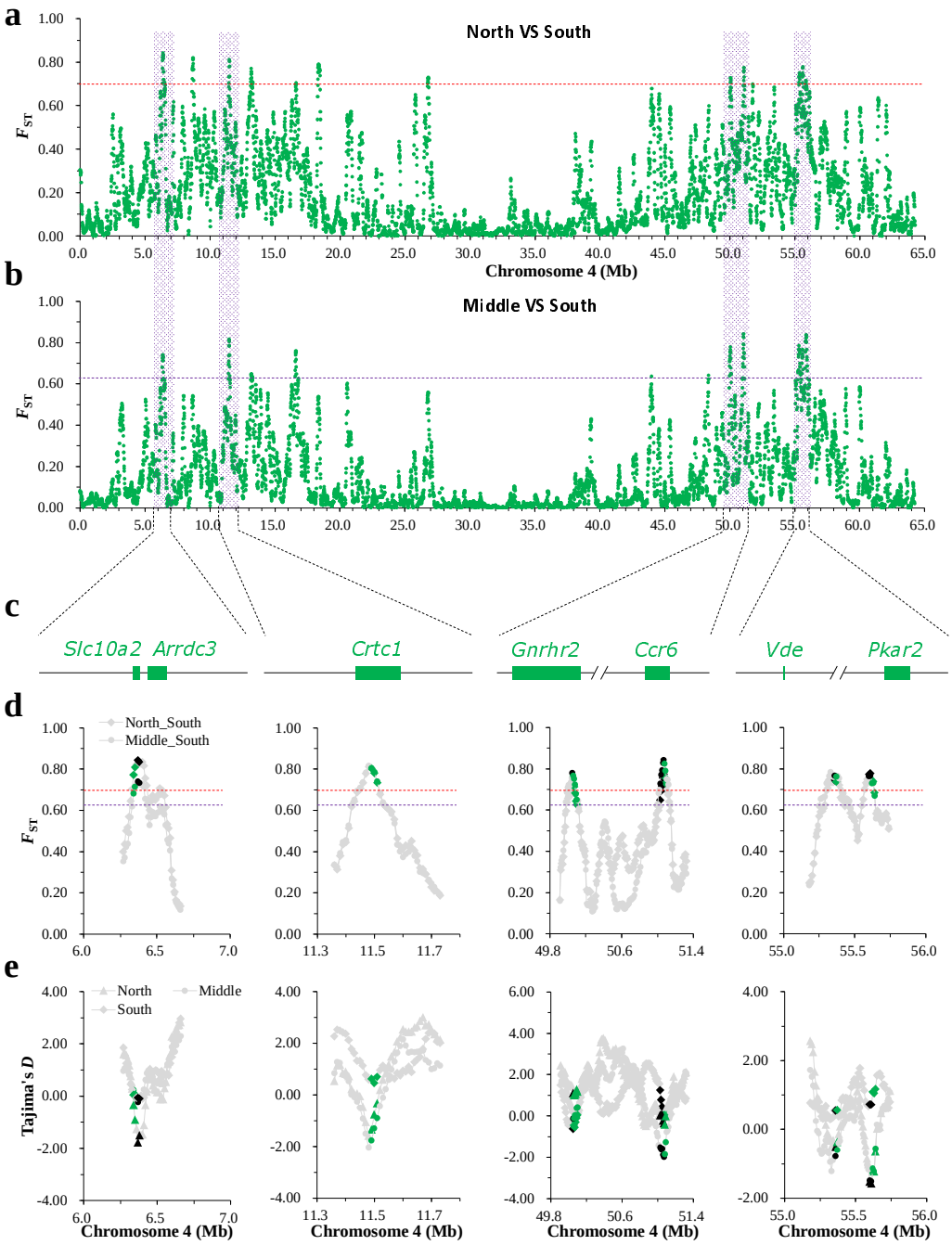

Fig. S10 | Signatures of selection along chromosome 4 in northern, middle and southern populations of the estuarine oyster. a and **b**, Selective sweep signatures identified by top 1% F_{ST} value (dash lines) between northern and southern populations (**a**), and between middle and southern populations (**b**). **c**, Models of annotated genes located within selective regions along chromosome 4. **d**, F_{ST} values surrounding selective regions om chromosome 4 between population pairs. **e**, Tajima's *D* surrounding selective regions on chromosome 4 in northern, middle and southern populations. Noncoding regions were marked with black, and coding regions were green.

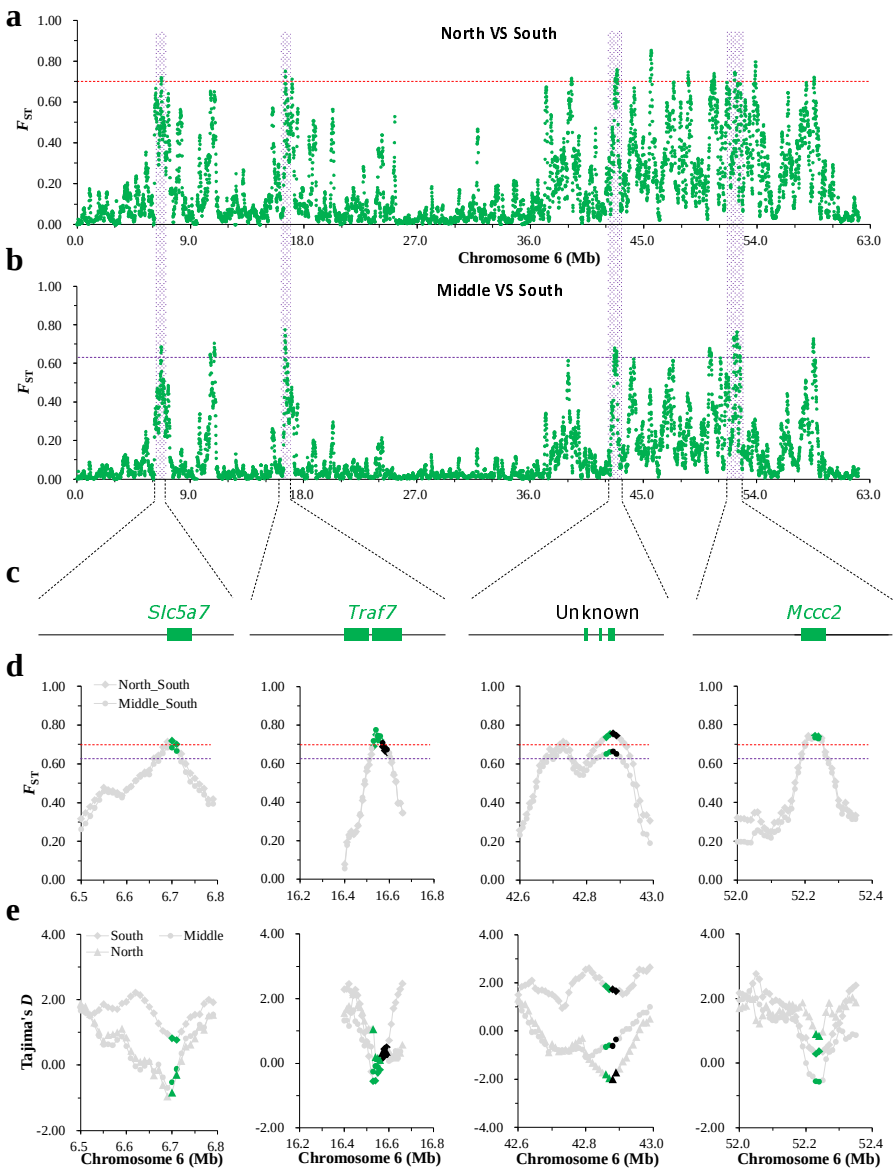

Fig. S11 | Signatures of selection along chromosome 6 in northern, middle and southern populations of the estuarine oyster. a and **b**, Selective sweep signatures identified by top 1% F_{ST} value (dash lines) between northern and southern (**a**), and between middle and southern populations (**b**). **c**, Models of annotated genes located within selective regions along chromosome 6. **d**, F_{ST} values surrounding selective regions om chromosome 6 between population pairs. **e**, Tajima's *D* surrounding selective regions on chromosome 6 in northern, middle and southern populations. Noncoding regions were marked with black, and coding regions were green.

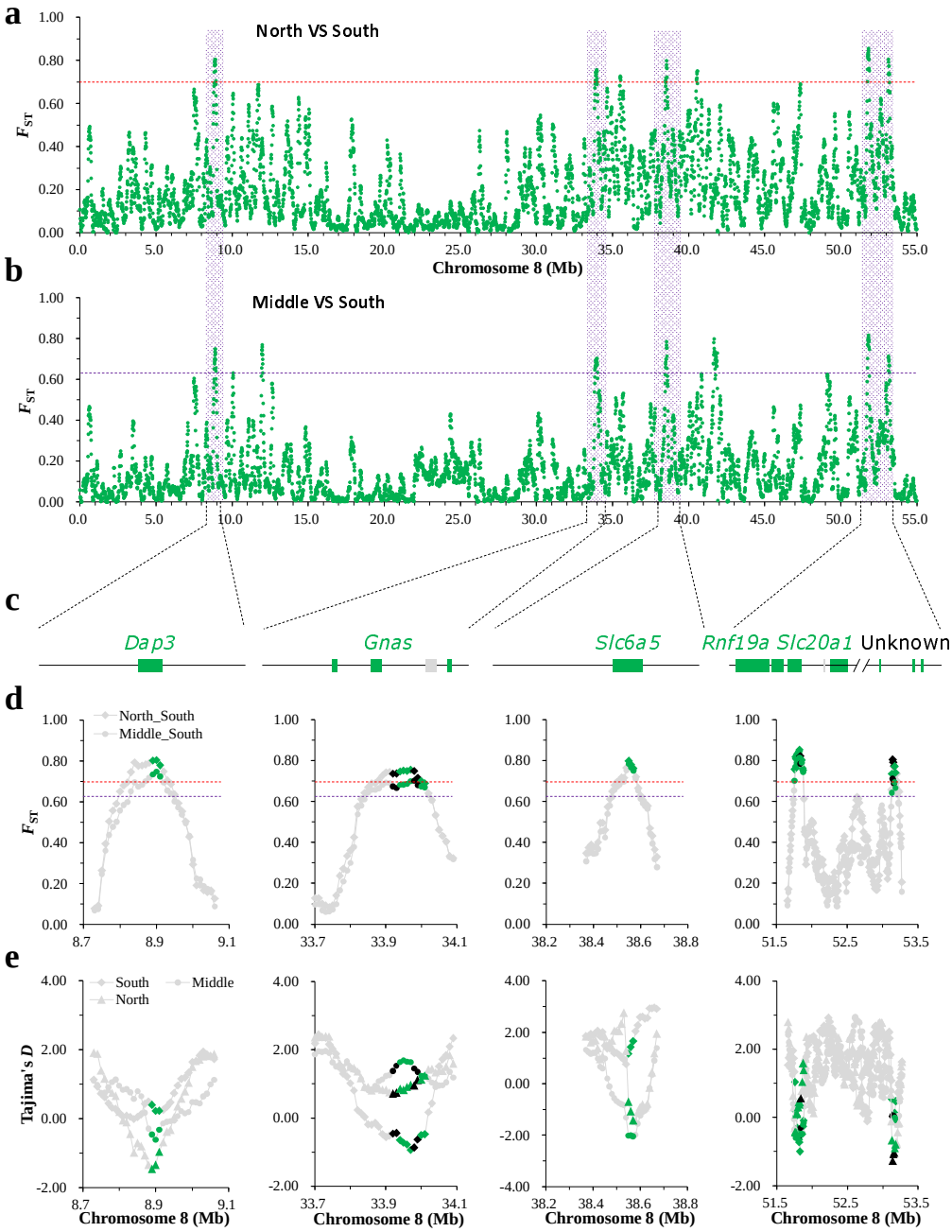

Fig. S12 | Signatures of selection along chromosome 8 in northern, middle and southern populations of the estuarine oyster. a and **b**, Selective sweep signatures identified by top 1% F_{ST} value (dash lines) between northern and southern (**a**), and between middle and southern populations (**b**). **c**, Models of annotated genes located within selective regions along chromosome 8. **d**, F_{ST} values surrounding selective regions om chromosome 8 between population pairs. **e**, Tajima's *D* surrounding selective regions on chromosome 8 in northern, middle and southern populations. Noncoding regions were marked with black, and coding regions were green.

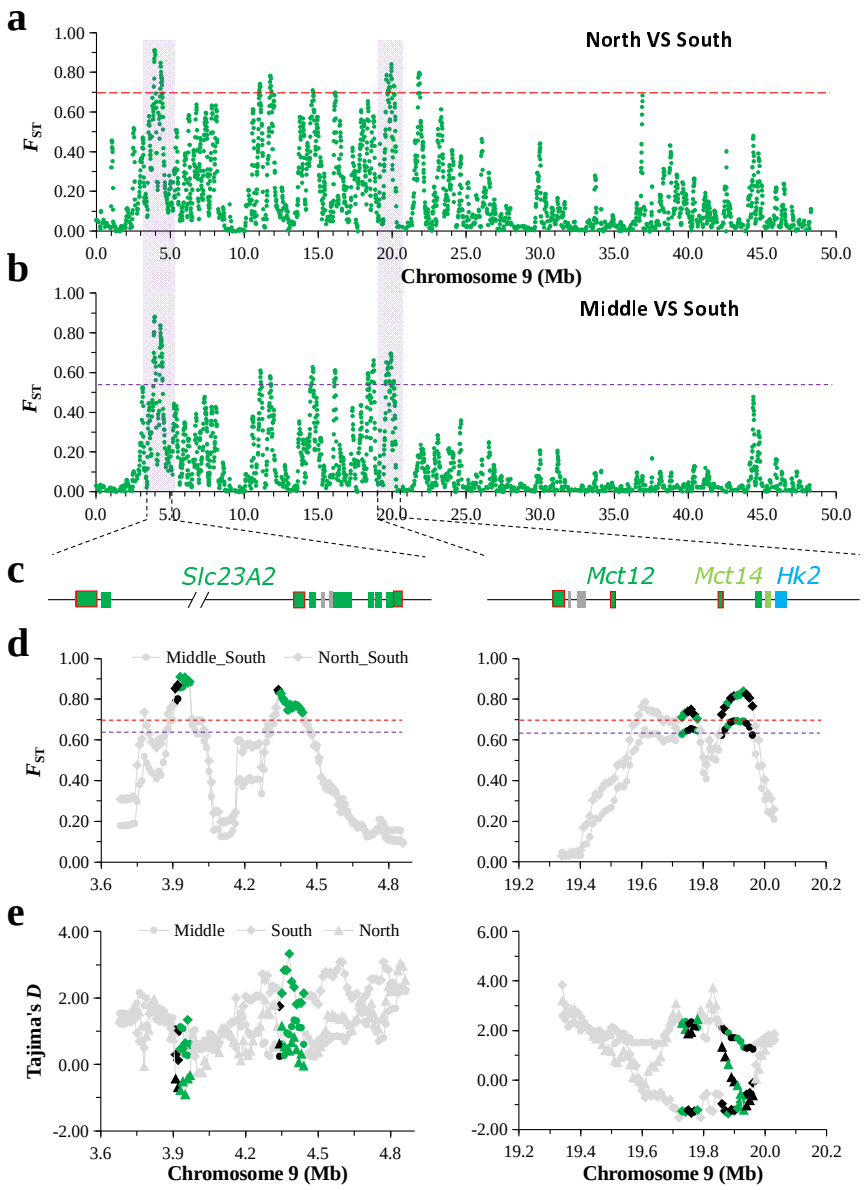

Fig. S13 | Signatures of selection along chromosome 9 in northern, middle and southern populations of the estuarine oyster. **a** and **b**, Selective sweep signatures identified by top 1% F_{ST} value (dash lines) between northern and southern (**a**), and between middle and southern populations (**b**). **c**, Models of annotated genes located within selective regions along chromosome 9. Models with red lines are responsive to temperature and salinity challenges. **d**, F_{ST} values surrounding selective regions om chromosome 9 between population pairs. **e**, Tajima's *D* surrounding selective regions on chromosome 9 in northern, middle and southern populations. Noncoding regions were marked with black, and coding regions were green.

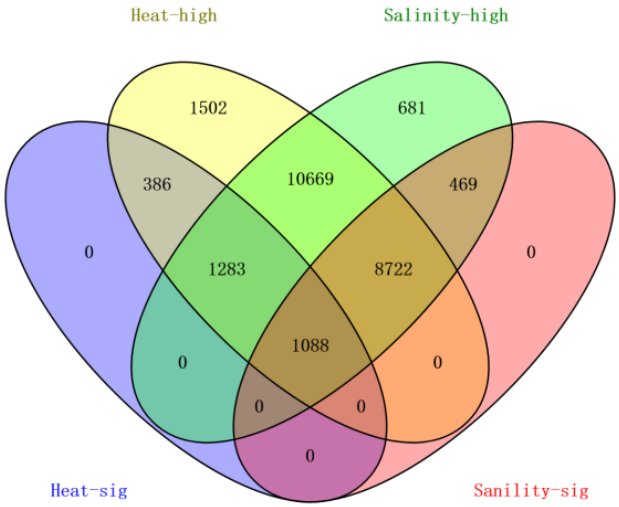

Fig. S14 | Venn diagram of genes expressed in response to high temperature and high salinity stresses in the estuarine oyster. Heat-high and salinity-high indicate genes expressed under elevated temperature (6 hours under 37□ seawater) and high salinity (7 days under 60‰ seawater) excluding genes with low expression. Heat-sig and salinity-sig indicate genes significantly up- or down-regulated in response to high-temperature and high-salinity stresses.

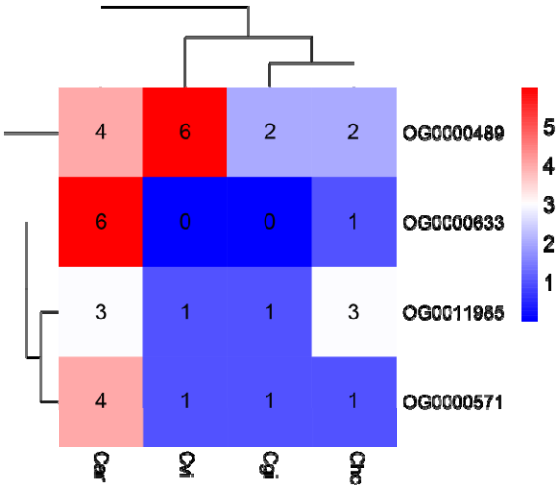

Fig. S15 | Copy numbers of orthogroups of *Slc23a2* and *Mct12* gene families in four *Crassostrea* oyster species. OG0000633: uric acid transporter, OG0011985 and OG0000489: purine permease, OG0000571: purine efflux pump. Cvi: *C. virginica*, Car: *C. ariakensis*, Cho: *C. hongkongensis* and Cgi: *C. gigas*.

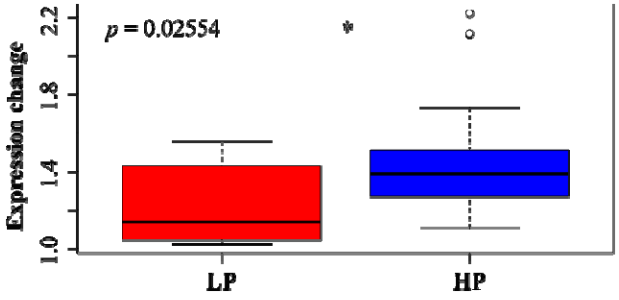

Fig. S16 | Expression changes of estuarine oyster genes showing low plasticity (LP) and high plasticity (HP) when reciprocally transplanted to non-native habitats.